2006

EXPERIMENTAL STUDY AND QUANTIFICATION OF EMISSIONS IN CONTROL ATMOPSHERE BRAZING PROCESS

Ajay Babu Renduchintala
University of Kentucky, arend2@uky.edu

ABSTRACT OF THESIS

EXPERIMENTAL STUDY AND QUANTIFICATION OF EMISSIONS IN CONTROL ATMOPSHERE BRAZING PROCESS

The work explains how the dynamics of the release of water vapors from flux during the Control Atmosphere Brazing influences the process conditions important for the quality of the brazed product. The process involves sequential events such as continuous ramp-up heating, flux and filler melting, reactive flow, isothermal dwell and rapid quench solidification performed under the controlled atmosphere. During this complex process effluents are released. Some effluents are detrimental for the product quality (water vapor) and some are harmful for the environment (HF). We selected to study water vapor emissions with an objective to quantify these emissions and to consider their influence on the manufacturing process.

Experiments were conducted using different fluxes. Findings are presented to compare the vapors released in each case. The objective is not necessarily to develop a metric for sustainability, but to understand the kinetics of an effluent release. A simple predictive model has been devised to approximate experimental data behavior. The data from the TGA analysis obtained from other sources, and the dew point temperature history from the controlled atmosphere brazing experiments performed in course of this work, have been used for the purpose of comparison and analysis.

KEYWORDS: Control Atmosphere Brazing, Effluents, Flux, Dew point.

Ajay Babu Renduchintala

September 25th, 2006

EXPERIMENTAL STUDY AND QUANTIFICATION OF EMISSIONS IN CONTROL ATMOPSHERE BRAZING PROCESS

By

Ajay Babu Renduchintala

Dr. Dusan P. Sekulic

(Director of Thesis)

Dr. I.S. Jawahir

(Director of Graduate Studies)

September, 2006

RULES FOR THE USE OF THESIS

Unpublished thesis submitted for the Master's degree and deposited in the University of Kentucky Library are as a rule open for inspection, but are to be used only with due regard to the rights of the authors. Bibliographical references may be noted, but quotations or summaries of parts may be published only with the permission of the author, and with the usual scholarly acknowledgements.

Extensive copying or publication of the thesis in whole or in part also requires the consent of the Dean of the Graduate School of the University of Kentucky.

A library that borrows this thesis for use by its patrons is expected to secure the signature of each user.

Name Date

THESIS

Ajay Babu Renduchintala

The Graduate School

University of Kentucky

2006

EXPERIMENTAL STUDY AND QUANTIFICATION OF EMISSIONS IN CONTROL ATMOPSHERE BRAZING PROCESS

THESIS

A thesis submitted in partial fulfillment of the requirements for the degree of
Master of Science in Manufacturing Systems Engineering from the
College of Engineering at the University of Kentucky

By

Ajay Babu Renduchintala

Lexington, Kentucky

Director: Dr. D.P. Sekulic, Professor
Center for Manufacturing, Department of Mechanical Engineering
Lexington, Kentucky
2006

Dedicated to my Parents….

ACKNOWLEDGEMENTS

This work would have not been possible without the diligent supervision and long discussions with my advisor Dr. Dusan P. Sekulic. I would like to thank him for including me into the project team working on a study of a brazing process. The perfection he seeks in every little detail helped me to develop my presentation and writing skills.

I would like to thank Mr. Matthew Guzowski from KB Alloys for providing me data on brazing flux physical characteristics. Also my thanks go to Dr. Hui Zhao for helping me to conduct all the experimentation included in the thesis. The advice and suggestions provided by my fellow graduate students have been of a tremendous help in organizing the material. I sincerely thank Dr. I.S. Jawahir for his support in the Fall 2005, providing me an opportunity to be his teaching assistant which sharpened my teaching skills. I thank Dr. Marwan Khraisheh and Dr. Jawahir to be on my defense committee.

TABLE OF CONTENTS

LIST OF TABLES

LIST OF FIGURES

LIST OF FILES

1. Thesis. PDF

NOMENCLATURE

r	Rate of reaction $(\mathrm{kg/m^3\,sec})$
k	Reaction constant $(\mathrm{sec^{-1}})$
C_{H_2O}	Concentration of water vapors (mol/m^3)
$C_{(H_2O)_0}$	Initial concentration of water vapors (mol/m^3)
W_{in}	Initial mass of the flux (kg)
W_t	Instantaneous mass of flux (kg)
t	Time (sec)
$\dot{V}_g$	Instantaneous volumetric flow rate of nitrogen gas mixture (m^3/sec)
$\dot{V}_{g,0}$	Initial volumetric flow rate of nitrogen gas mixture (m^3/sec)
ψ	Specific humidity
$\dot{m}_{H_2O}$	Instantaneous mass flow rate of water vapors in furnace chamber (mg/hr)
$\dot{m}_{H_2O,0}$	Initial mass flow rate of water vapors in furnace chamber (mg/hr)
$\dot{m}_{N_2}$	Mass flow rate of nitrogen gas (mg/hr)
M_{H_2O}	Molecular weight of water vapors (kg)
M_{N_2}	Molecular weight of nitrogen gas (kg)
ρ_{N_2}	Density of nitrogen gas (kg/m^3)
P_v	Partial pressure of water vapors (N/m^2)
P_s	Saturated vapor pressure (N/m^2)
P	Pressure inside the chamber (N/m^2)
T_d	Dew point temperature (^0C)

CHAPTER I

INTRODUCTION

1.1 Background and Motivation

There has been relatively little published analytical research and modeling devoted to determination of the impact of effluents on the quality of brazing in the context of sustainable engineering. In particular, little or no published information is available about the kinetics of the process and its modeling. To study the dynamics and the modeling aspects, we have selected Control Atmosphere Brazing (CAB). The quality of the process / product can be described in terms of different figures of merit. In our study we will analyze some features of the brazed joint topology responsible for the integrity of the joint, for example the length of the fillet formed in a specially designed test. These studies will be directed toward understanding influence of the kinetics of the process effluents.

The joint formation depends on the capillary flow of the filler metal towards the joint. The flow is facilitated by the surface tension action. This flow is hampered due to the existence and the formation of aluminum oxide (Al_2O_3, alumina) on the surface of the mating surfaces. This Al_2O_3 formation is enhanced (therefore, wetting reduced) by the reaction between: (1) the oxygen from the surrounding atmosphere, (2) the flux and (3) the mating surfaces. The water vapor and/ or the oxygen content that is present in the furnace chamber reacts with mating surfaces to form oxide and at the same time with the flux. The oxide formation leads to poor wetting of molten metal over substrate. Therefore, the filler metal would not flow towards the joint area and the joint formation would become poor.

As a result of this realization, a clear direction for a R&D effort can be formulated: Dependence of the product quality on the H_2O effluents indicates a need to analyze effluents formation and influences on the joint formation. It is apparent that it is important to study the chamber atmosphere that surrounds the brazed part throughout the brazing process. Quantitative parameters have to be identified to monitor the state of the surroundings and its effect on the brazing process. Most of the past studies, for example, [50] [62] considered oxygen content as the important parameter. The research done by the Claesson [13] involved monitoring of the content of oxygen in the furnace atmosphere. The aim was to maintain oxygen at low but consistent levels. This is in particular important because the oxygen concentration in the furnace increases as the process advances to the later stages. The reason for these increased levels can be related to different phenomena. The research performed by Field, Liu and Terrill [1] [2] [4] also indicated that the oxygen content is increased due to the release of water vapors from the flux used in the process. The flux used in that study is Nocolok® flux and its derivatives.

The dew point temperature within the furnace chamber has also been extensively controlled in industry. Dew point temperature in a furnace signifies the amount of water vapor that is present in the gas mixture. The work conducted in this thesis summarizes the information obtained through a series of CAB tests. Sequential changes of the humidity content expressed by the dew point level due to the presence of water vapor in the background atmosphere were registered. A hypothesis is adopted stating that the dew point temperature history is primarily the result of the release of molecularly bonded H_2O in the flux used in the process. The related chemical reactions responsible for the release of the water vapors and their interactions with the base metal and the flux in forming/ destructing the alumina are listed as well.

1.2 Objective

The objective of the work is

- To perform the literature review about the flux – aluminum substrate chemical reaction mechanisms that results in the release of water vapors and other effluents during the brazing process.
- To experimentally demonstrate that the dew point is an important parameter in the CAB process evaluation and to analyze the behavior/ history of the dew point vs. quality of the joint.
- To elaborate on the hypothesis that the water vapors are generated primarily from the flux used in the brazing process.
- To discuss important parameters which have the potential to reduce the emissions of water vapor during a CAB process.

1.3 Layout of Thesis

The first chapter offers a brief description of the process known as the Control Atmosphere Brazing (CAB) and lists explicit statements on the background, motivation and objective of the research. The second chapter offers a literature review explaining the set of chemical reaction mechanisms responsible for effluents release during the process. The mechanism of the aluminum oxide formation and the role of flux in safeguarding the quality are briefly discussed. Details of the performed CAB experiments are presented subsequently. The analysis of the importance of monitoring the dew point temperature level on the quality of brazing is discussed next.

The third chapter presents experimental data. This chapter is the central point of the Thesis. The main objective has been to gather a set of data that illustrates dew point temperature history for a real aluminum brazing process. In addition to recording the process data, experimentation conducted is performed on a set of brazed "wedge-tee" samples to analyze the product quality.

A simple model intended to simulate emissions of H_2O resulted from the chemical changes occurring in the flux with the advancement of the heating cycle is presented in fourth chapter.

The fifth chapter presents the data generated during experimentation involving variability of imposed ramp rates and the results of the analysis of the impact of ramp-rates in reducing the vapor emissions. This chapter also offers a partial insight into the relation between quality and water vapor emissions.

The sixth chapter provides conclusions and summarizes the final outcomes from the experimental work and modeling.

CHAPTER II

LITERATURE REVIEW

2.1 Sustainability and the Life Cycle Assessment of a Manufacturing Process

Maintaining ecological balance is very important keeping in view the costs incurred due to the disasters prompted by disturbances of sustainability. The research performed by Glasby et al [63] confirmed that in the last few decades the frequency of natural disasters has considerably increased. This is mostly credited to the green house gases. According to Glasby et al [63], as the percentage of these gases (e.g. carbon-dioxide, sulphur-dioxide etc) increases, the global warming increases which ultimately results in the more frequent appearance of cyclones, heat waves, bush fires etc. That study concluded saying that the long term costs involved in decreasing these emissions are much lesser compared to the resurrection costs [63]. This calls for the quick and efficient ways to improve the environmental sustainability. Although not all authors agree on the actual cause-consequence of events, multiple studies indicate that man inflicted impact is real [18]. For example, the serious issue concerning semi-conductor manufacturing industry was the use and emissions of Perfluorocompounds (PFCs) [19]. Study conducted by Walsh [20] indicates the increase in sales of diesel fuel would lead to relative high NOx and particulate emissions which are of major pollution concerns for many countries across the world [20].

It is apparent that there are many contributors of the emissions, like automobiles, manufacturing industry, pharmaceutical emissions etc. One of the possible ways of getting the situation under control is to monitor the gases coming out of the manufacturing processes and improve the processes based on the available feedback. Many studies concerning emissions from automobiles are concentrating on reducing the total weight of the vehicle body so as to decrease the fuel consumption and thereby the

releases [20]. Industrial processes like welding, brazing, casting, forging; all are involved with emissions of these gases. These phenomena might cause a potential harm to the immediate surroundings. The resulting losses can be observed in the form of air, water or land pollution. There is a chance that the humans and other living beings getting in contact with these emissions may be affected in negative way as well.

Metal joining processes like welding and brazing are important trades employing 700,000 and 400,000 in US and Japan respectively [16]. It has been reported that a number of pulmonary irritants such as Hydrogen Fluoride and Boron-tri-Fluoride (HF and BF_3) are produced as a result of brazing [15]. These operations produce gaseous and aerosol by-products composed of complex array of metals, metal oxides and other species volatilized from the base metal, the welding electrode/ filler metal or the fluxing material [16] [17]. In conclusion, one may easily emphasize that these effluents are very important in controlling the ecological problems such as global warming.

In some of the brazing process segments, the resulting emissions can be from the intermediate stages which may cause harm to the ultimate interests of the process. This, in return, affects the product quality and incurs losses. For example, the water vapor released in the mid stages of the brazing process results in the formation of alumina (Al_2O_3) which, as we already emphasized in Chapter 1, hampers the capillary effects and hence influence the product quality. In addition, the presence of H_2O vapor leads to the production of HF vapors [1]. Studies were conducted across United States and rest of the world to estimate the impacts of manufacture, use, transport and storage of HF near the residential areas [21]. Terrill [4] concluded that the black spots formed on the surface of the part are also a result of the deposition of HF during the process.

2.2 Brazing and Sustainability

Brazing is a joining method in which different metals and non-metals can be joined with or without using the flux [22]. Involvement of flux is very common in the Control Atmosphere Brazing method which is a state-of-art joining method employed in various

automotive, aeronautical, refrigeration, air-conditioning and many other sectors. High temperature control atmosphere brazing is extensively used to join structural steels and super alloys [23]. Using this method, complex multi-joint assemblies can be economically manufactured resulting in a fine quality to sustain structural and thermal stresses. The sustainability issues involving this process and products are both the environmental and economical in nature. The HF vapors are ecologically dangerous while water vapors are the prime source for the formation of HF and hindering the product quality [4].

The melting point of the filler metals in brazing is above $450^{0}C$ as established by a convention [22]. The filler metals possess lower melting points than that of the base metal. So the joining is performed without melting of the parent metal. In the case of furnace brazing such as CAB, heating can not be limited to targeted local joining positions. That is, the whole assembly must be processed, including flux deposition on large product surface areas, hence leading to an increase in effluents increase. The filler metal required for joining can be provided in different forms like wires, rods, coils etc. At high temperatures, this filler metal melts and flows towards the joint due to the capillary action [23]. A good braze filler metal should possess excellent capillary flow characteristics; relatively low braze temperatures, low susceptibility to oxygen and good joint strength/ductility [22]. Besides selecting a good filler metal, care should be taken to see that the surface on which the molten filler material is supposed to flow should be chemically cleaned from the contaminating surfaces such as oxides, dirt, grease, etc [25].

The quality of a brazing joint is equally dependent upon the filler metal state, and if deposited as a paste its powder size is important [26]. When performing a brazing process with the air-atomized powders and argon-atomized powders, the powders with less oxygen content were found more suitable for brazing. The reason was they consumed low amounts of flux to form a sound joint. In addition to: (1) the proper selection of good braze filler metals (to have a free molten metal flow), (2) flux to remove the surface oxide films, and (3) appropriate fixture design, there are lot of other conditions which need to be kept under control to form a good quality joint. For example, proper controlled

atmospheres should be provided in order to avoid oxidation; lower dew points should be maintained within the chamber. For example, research performed by Claesson [13] demonstrated the use of a computer feed back system from the CAB chamber to vary the nitrogen flow according to the oxygen content present.

As seen above, there are a lot of sustainability issues related to quality involved in the brazing. Also the ecological concerns (for example, emissions of HF) are also very important as discussed above. HF vapors can cause dermatological problems and are harmful to eyes. In order to develop strategies for mitigating the above mentioned sustainable issues, control of the vapors (both water vapor for quality and HF for pollution) is an immediate and important assignment.

2.3 Control Atmosphere Brazing

Controlled Atmospheric Brazing (CAB) is a state-of-art process developed by Alcan (US Patent: 3951328), [62], under the trade name Nocolok®. It is a non-corrosive flux brazing process which is widely used in the manufacturing of heat exchangers. The advantage of this process is that cleaning of the flux residue is not needed. The process involves the use of clad/core brazing sheet. The brazing sheet represents a two or multi layered composite of at least two distinct aluminum alloys [34].

The clad layer located on one/both sides of the aluminum sheet represents only a small amount of total sheet mass. The layer thickness is usually up to 10 % of the total sheet thickness. This layer is made of Al-Si alloy that has a lower liquidus temperature than that of the substrate, say Al-Mn alloy. The clad is attached metallurgically to the base metal. At elevated temperatures, cladding melts and subsequently wets the mating surfaces to be bonded, ultimately leading to joint formation if an efficient removal of aluminum oxide layer from the surface is secured. A very short duration of the critical phase of the cladding melting and molten metal flow (the duration of this phase is of an order of magnitude of $(10^{-1}$ to 10^{0} sec$)$ [34], a precisely defined and a very narrow temperature range (say, between 870 and 890 K), and a rigorously controlled gas

atmosphere (say, a high-purity nitrogen, 99.999 %, with less than 100 ppm of oxygen during brazing, and extremely low dew point temperatures of up to -40 ^0C and lower), make any study of these phenomena difficult under conditions of actual technological applications. The process is complex due to the inevitable presence of an oxide layer that covers cladding. The oxide as explained before, if not efficiently removed hinders the wettability of the metal surfaces and prevents free flow of the melted micro layer into the joints. Consequently, a flux must be used.

Flux used in a state-of-the-art brazing process is a eutectic mixture of $KAlF_4$ and $K_2AlF_5 \bullet H_2O$. This flux was invented in the 1960's and since then it has been extensively used in aviation, chemistry, military, instrumentation, machinery, industries and so on [27]. Nocolok® flux is now a registered trademark of Solvay Fluor. This flux can be used not only for the furnace and for the flame brazing applications, but for the induction applications too [51]. Also, this flux can be used for large and small volume of productions. It is a non-corrosive brazing agent. The main characteristic of this flux is a low melting point, but close to the melting point range of clad. In general the melting point of this eutectic mixture (a molar ratio of AlF_3 to KF = 44.5: 55.5) is found to be 565 ^0C [28] [29]. It is known that the melting point of the substrate if made of pure aluminum is 660 ^0C but can be significantly reduced if an alloy is considered. It would be very difficult to obtain a sound joint if the melting points of flux, clad and the aluminum alloy substrate are very close to each other. For a given aluminum alloy material the melting point of the substrate is relatively high and a good joint can be obtained for Al+Si clad. One way of lowering the melting point of the flux eutectic, is to add a third element (for example magnesium, indium and zinc) into the flux during its preparation [58].

The research performed by Zhang et. al. [30] explored the influence of reaction temperatures during the preparation of flux on the lowering of melting points. They concluded that with the rise of reaction temperatures during the preparation of the flux, its melting point was lowered considerably. For a good homogenous joint, the melting

point of the flux is between 560^0C and 565^0C which could be obtained processing flux compounds at 100^0C reaction temperature. The melting point of the clad, Al-Si alloy is 577^0C (solidus), just above the melting point of the flux. Kawase H., et al. [62] explored the impact of mixing ratios between $KAlF_4$ and $K_2AlF_5 \bullet H_2O$ on the formation of good joints. Studies reported that the composition of $K_2AlF_5 \bullet H_2O$ less than 20% of the total mixture resulted in a poor joint. The compositions between 20 and 40 percentages were found to form excellent joints whereas with the percentages more than 65 resulted in the poor joints [62].

The main aim of the flux is to disturb the existing layer of aluminum oxide on the surface and to prevent its formation on the substrate during the later stages of the process. Apart from very thorough metallurgical and/or mechanical characterizations of various brazed materials, as well as some details of physical chemistry of the process important for manufacturing aspects of the brazing technology [34], little is known about the physics of the flow of the molten aluminum alloy micro layer, and in particular, about the joint formation that follows immediately after the molten alloy flow phase. This is true for the controlled atmospheric brazing as well.

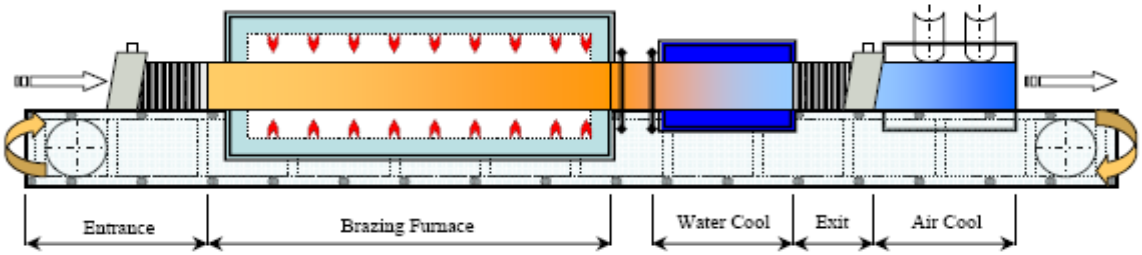

Fig. 1 Typical Controlled Atmospheric Brazing Furnace [52] [59]

The filler metal (if brazing sheets are not used) is typically placed adjacent to or in between the components to be joined and the assembly is heated to a temperature where the cladding material melts (but the parent material does not). The process is accomplished in a continuous CAB furnace Fig. 1. Upon cooling, the cladding forms a metallurgical bond between the joining surfaces of the component. The aluminum

brazing process under controlled atmosphere in industry occurs in a furnace, (see Fig. 1), usually under the following process parameters [52] [59]:

- Operating temperature 853 K to 893 K
- Part Temperature Uniformity of ±3 K
- Nitrogen atmosphere with dew point <-40 ^0C and the small oxygen content <100ppm
- Flux density 5-15 g/m^3

As indicated earlier, the cladding of the brazing sheet is supplied via a thin layer, metallurgically attached to the base alloy. The base alloy provides the structural integrity while the low melting point cladding melts to form the brazed joints [52]. The atmospheric conditions in mass production of aluminum brazed products, say automotive heat exchangers are accomplished through the use of nitrogen, which is readily available.

A radiation heating CAB furnace, as shown in Fig. 1, is an ideal facility for brazing similar size products in a continuous flow environment. If one intends to produce a single type or only a few variations of a product in large numbers, a radiation furnace system makes sense (for example 60radiators/hour or 60condensers/hour). The furnace is designed to use a stainless steel muffle, supplied with the nitrogen atmosphere and to provide uniform heating of the products. The heat input into the furnace chamber is controlled through electric heating elements or natural gas fired burners to heat muffle which in turn heats the products [52].

Today, more than 400 CAB furnaces are in operation throughout the world using the Nocolok® process [52]. This technology offers the benefits of flux utilization for successful oxide removal and operation at atmospheric pressure while avoiding the disadvantages of post braze treatments and corrosion susceptibility. The process in most brazing operations includes the following steps [52]:

- Component forming and assembly
- Cleaning and flux application
- Brazing
- Post brazing procedures

The typical process steps involved in aluminum brazing are the furnace bake-out, continuous ramp-up heating till the peak temperature of brazing, dwell period and the quench. The bake-out is done by allowing the inert gas (nitrogen) to flow through the hot zone continuously. This helps in removing out all the water vapor and oxygen content present in the chamber. In general practice, the start of the brazing is prompted by monitoring the oxygen level and the dew-point temperature in the chamber. The process sequence in brazing operations for mass production of, say, heat exchangers, is depending on [60]:

- Heat exchanger design
- Cleaning method
- Flux application method

Success or failure in CAB production relies on several factors [52]. The starting point is good product fit-up. Parts to be metallurgically joined must have intimate contact at some point along the joint. An adequate quantity of filler metal, but not an excessive amount must be available to fill the joints. Intimate contact is recommended, when clad products are used. Another essential basis for reliable brazing results is a uniform flux coating on all surfaces involved in the joint formation [4]. The main focus for achieving this task is cleaning and fluxing procedure. Equally important are the furnace conditions, i.e. temperature profile, temperature uniformity, and atmosphere conditions.

In the ramp-up heating process, the sample is heated from room temperature to the peak temperature ($600^{0}C$). Normally this heating takes place for about 10 - 12 minutes (a bit longer with thermal degreasing). It is at the end of this period, the clad melts and flows towards the joint area. The subsequent quench is the rapid cooling of the joint. The brief

description of the laboratory system used in the research, as opposed to an industrial facility, Fig. 5, is given in Chapter 3.

The dynamics of chemical reactions involved in the release of vapors and the formation of oxide layer is very important to study. The flux Potassium-Fluoro-Aluminate (Nocolok®) can be roughly described with [1] [4] [30]

$$K_2AlF_5 \bullet H_2O + KAlF_4 \tag{1}$$

Note that the oxide layer may be formed due to the presence of oxygen in atmosphere and water molecules that get dissociated during the heating of the potassium fluoro-aluminates compound. In the subsequent reactions, the water molecules react with the flux constituents to form HF and alumina [1] [4]. In the present work, the focus has been shifted to the water vapor emission coming out of the flux, and not to HF. The main reasons are

1. Presence of water vapor is one of the prime reasons for the formation of hydrogen fluoride. Also water vapor greatly affects the quality of the product.
2. Monitoring of water vapor can be performed by monitoring the dew point temperature and can be easily quantified.
3. Handling HF as a harmful substance requires special care, and separate equipment to study the release of HF with respect to temperature during the process, what is beyond the scope of this work.

Comparatively, it is relatively easy to observe the release of water vapors from a system as emphasized above. This can be done by using the sensors which can precisely measure the dew point temperature of atmosphere in the chamber.

A representative graph which illustrates the brazing cycle, i.e., (1) the heating ramp rates, (2) the dwell at the peak, and (3) the quench, as well as the dew point profile during a typical CAB process is given in Fig. 2. This process is executed within the experimental

program of this thesis in an experimental facility described in Chapter III. The fluxes used in a process were flux denoted as the 'S' type and additional modifications denoted as J, BC, N, Q, H, W, B12. Fig. 2 corresponds to the 'S' type. All the temperature and dew point history is present in the file named 'Sample S' were on CD attached to the report. Prior to the experiment, the heating chamber of the apparatus is baked out by allowing Nitrogen gas to flow through it, to obtain the required low initial dew point at the onset of test series and to secure a very low oxygen content within the chamber. From the graph in Fig. 2, we can observe the heating rate is increased at a steep rate around $39^0 C/\min$ to reach the peak temperature of brazing which is at $601^0 C$. At the peak temperature, there is a dwell i.e. the same temperature is maintained for 2 minutes. The environment composition within the chamber is of utmost importance at this peak (explore the dew point curve in Fig. 2). Care should be taken to prevent the formation of oxide layer on the surface which hinders the flow of liquid filler, hence although the dew point sharply increases first (due to the water molecules dissociation), subsequently the dew point sharply reduces, being replaced by nitrogen.

In a typical industry setting, the water vapor in the chamber could be present due to various reasons, (1) like the leakages from the cooling pipes, or (2) the moist air that is dragged in with the sample in addition to the presence of water molecules bonded to flux. A continuous netshape manufacturing cell through which the parts to be brazed flow (i.e. the cells devoted to warm up, ramp-up heating, dwell and the quench) may operate under the presence of leaks. But, in a typical laboratory setup, the above factors can be safely neglected.

One of the possible and strong arguments for sharp increase in dew point values, Fig. 2, is that the vapors are getting released from the flux itself; refer Eq. (1). Many studies [1] [4] have concluded that decomposition of the flux occurs around 350 K ($76.8^0 C$) resulting in the formation of water molecules.

$$K_2AlF_5 \bullet H_2O + KAlF_4 \rightarrow K_2AlF_5 + H_2O \qquad (2)$$

It can be observed from the graph in Fig. 2 that the onset of exponential increase of dew point is registered in the temperature zone around $80^0 C$ (around 200 seconds). Also, the

heating rate zone, the clad melt zone, the dwell and the quench zones during a typical brazing process are marked in the graph of Fig. 2.

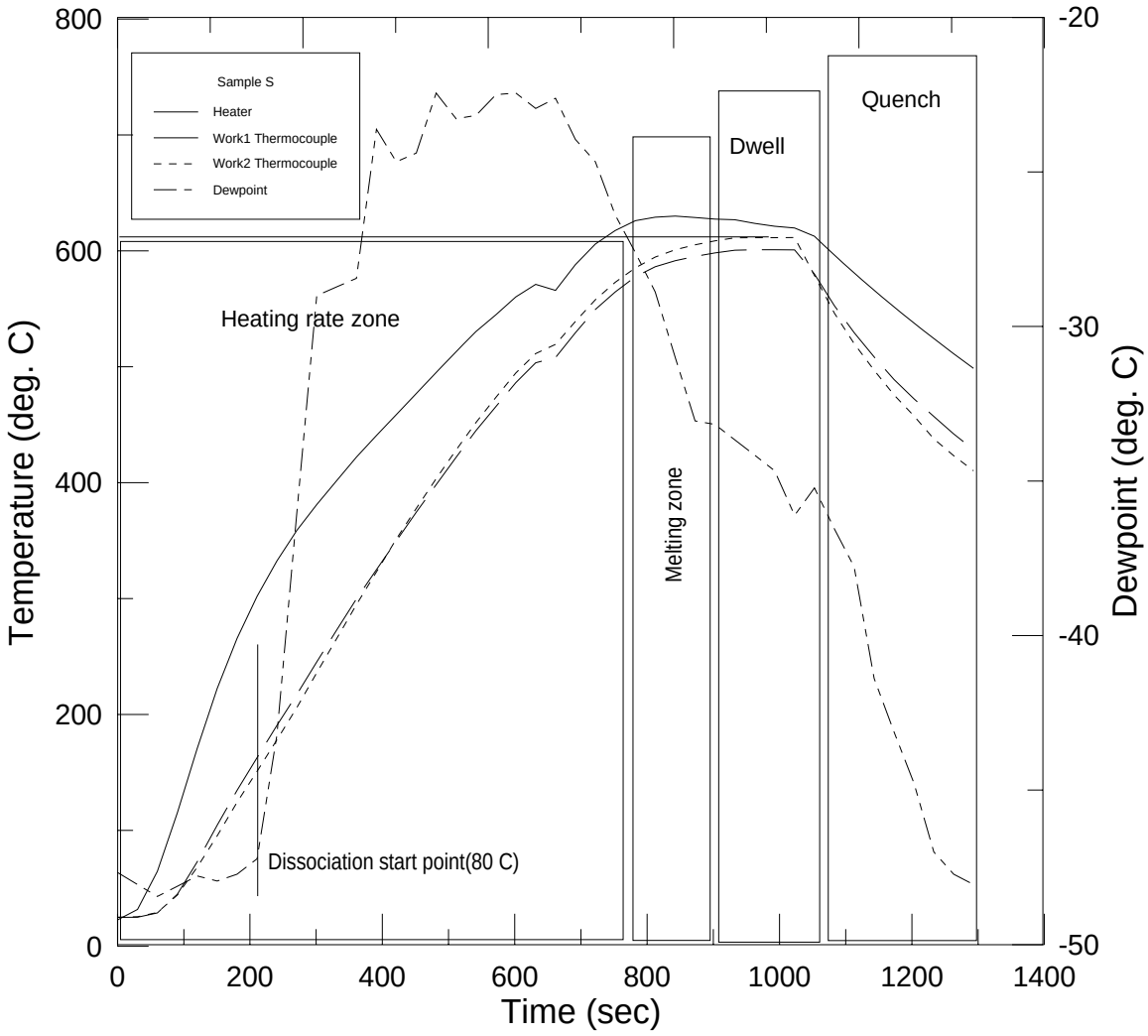

Fig. 2 Ramp-up heating History of Sample S in a CAB Process

The same exponential increase of emissions is also observed in a TGA analysis of the Nocolok flux; see Fig. 3 [11]. The data sheet named 'TGAS' is present on CD attached to report. Note, in the case of TGA experiments mass vs. time is registered, so an increase in emissions is actually registered as the decrease of the mass of the compound exposed to TGA (see Fig. 3). TGA analysis is a reliable thermal analytic procedure which involves monitoring of the weight loss of the sample in the chosen atmosphere (nitrogen or air) with respect to temperature. The comparison of the (1) weight loss from the flux (which

corresponds to the exponential increase of the released vapors) and (2) the exponential mass flow rate changes noted during the laboratory process once again affirms that the water vapors are released from the flux.

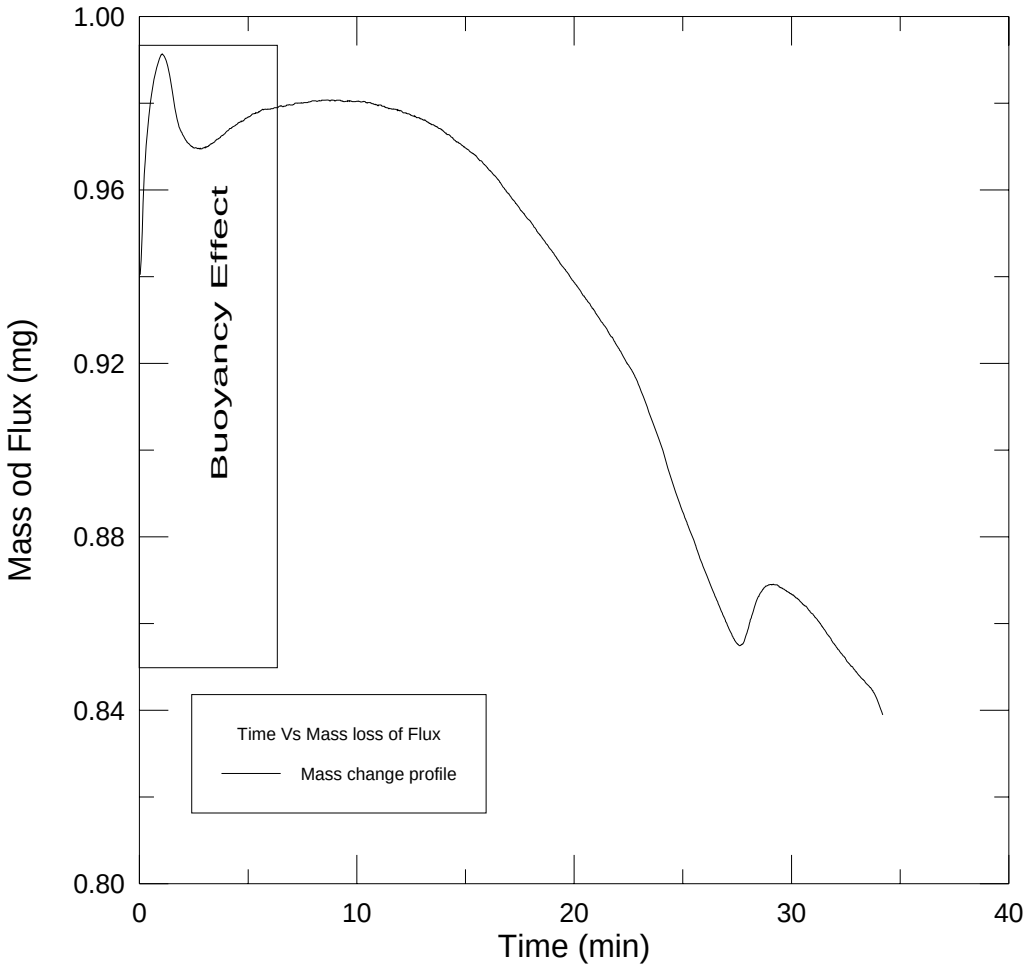

Fig. 3 Mass Change of Nocolok Flux in TGA-S Test

CHAPTER III

EXPERIMENTATION

3.1 Introduction

A series of CAB tests have been performed to analyze the humidity levels of the background atmosphere during brazing and joint formation. Different fluxes were used to conduct the experiments. Water vapor emissions from flux were closely monitored by measuring dew point temperature in the hot zone. The sample exposed to brazing in all tests was a wedge T-joint specimen which consists of two sheets arranged in perpendicular to each other. The vertical sheet is held at an angle to the horizontal sheet as presented in Fig. 4. This was made possible by balancing one end of the vertical sheet on a 1.6 mm diameter stainless steel rod. The vertical brazing sheet is held tightly to the base sheet (non clad) by a stainless or Nickel wire tied around.

The main idea of placing the vertical plate at an angle is to allow the formation of the brazed joint in the variable clearance gap formed in between the plates. The variability of the ultimate reach of the filler front for different samples signifies the variability in brazeability (i.e. wetting performance). The filler alloy on a brazing sheet is metallurgically bonded to the core of the metal sheet on both sides in the form of clad layers. As the heating cycle evolves the clad melts on the vertical sheet and flows towards the joint zone. The solidus temperature of the clad is 577 ^{0}C [1] just above the melting point range of the flux which is between 560 and 565 ^{0}C [1]. The flux consists, as indicated in Chapter 2, of potassium-Fluoro-Aluminate compounds. The actual melting range of these compounds depends upon the actual flux composition.

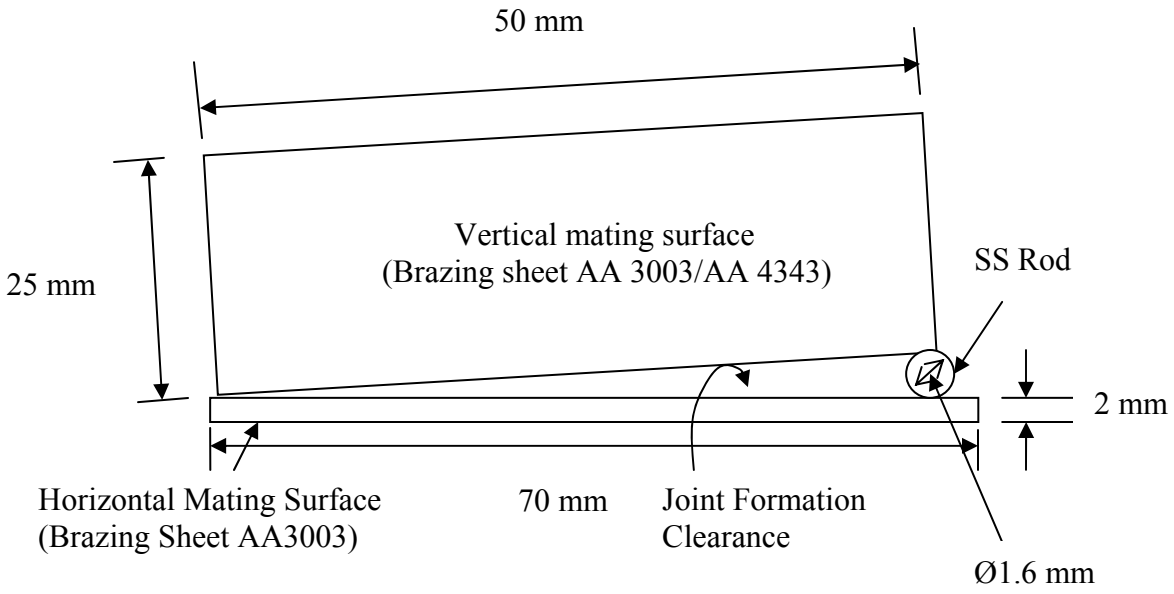

Fig. 4 Schematic Representation of a Brazing Sample

3.2 Sample Preparation

During the preparation of the sample, the vertical sheet of dimensions 50x25x0.5 mm (see Fig. 4) and horizontal sheet of dimensions 70x30x2 mm are cut from the original sheets. The stainless steel rod used is of 1.6 mm diameter. These sheets are ultrasonically cleaned in the first stage and later dipped in the ethyl alcohol and allowed to dry. Upon drying, both sides of the vertical sheet and the top surface of the horizontal sheet were coated with approximately the same mass density flux. The coating was facilitated either by using the spraying technique or by using the brush soaked with flux emulsion in Ethyl alcohol.

The amount of flux that has to be applied on the sheet must be precisely determined. Generally, it is considered that $5\,g/m^2$ of flux has to be applied [4]. In our case, the flux that has to be applied to a total surface of 0.00125 m^2 surface areas is around 25 mg. Care should be taken to measure the exact amount of flux to be applied on the surface. The weight of the brazing sheet is initially measured before applying the flux. Then the amount of flux mass calculated roughly according to the above mentioned procedure is

applied on the surface using a brush. The brush is dipped in the ethyl alcohol and then the flux is transferred onto the plate using it. After applying the flux on the surfaces, the weight of the sample is measured (after drying) again. The difference between the initial and final weights should give the exact mass of flux. A precise weight balance instrument is used to measure the mass. The weight measurement uncertainty was 0.1 mg.

The flux deposition results in relatively homogenous spread of the molten flux over the entire surface at the elevated temperatures. After the application of the flux, the vertical and the horizontal sheets are tied down together with a SS or Ni wire. In a similar manner, all the other samples are prepared by applying different fluxes. The dimensions of all the samples were kept unchanged.

3.3 Experimental Facility and Experimental Procedure

In parallel to the preparation of the sample, it is very important to get the CAB equipment ready and run tests consistently for different conditions. A typical experimental setup (see Fig. 5) is presented schematically in Fig. 6. The equipment consists of a central hot zone which is assembled from clear fused quart glass tubes. An advanced coating on the inner tube reflects heat back into the hot zone while simultaneously allowing visible light to pass through [60]. This efficiently insulates the furnace while providing an outstanding view of processes occurring within the hot zone. A clear fused quartz process chamber, located within the hot zone, provides a clean, dry, controlled atmosphere environment for the brazing process. The dimensions of the hot zone cylindrical volume are 4.5” inner diameter x 10” length.

This process chamber is equipped with the work platform on which the sample to be brazed is kept. This consists of a low cost, easily replaceable 304 stainless steel setter attached to it. This platform can be retracted from process chamber on linear slide for rapid and convenient sample change-out and thermocouple placement. This is connected to the end flange which is made up of hard anodized aluminum flange [60]. This flange is

sealed to the process chamber through o-ring seals. This flange acts as an entry for the special glass light rod and work thermocouples.

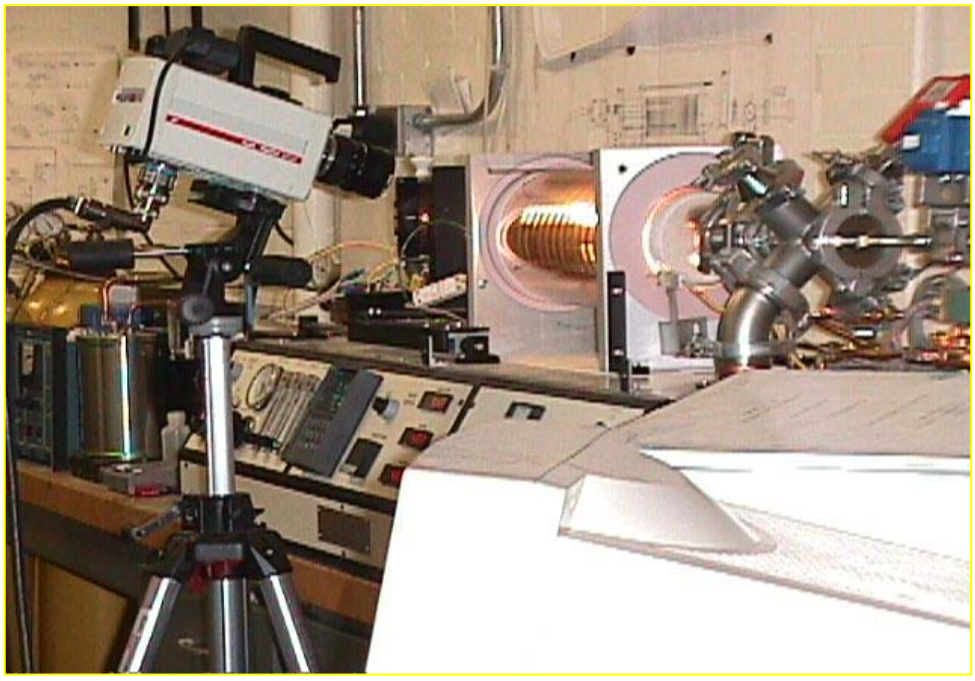

Fig. 5 Laboratory Setup

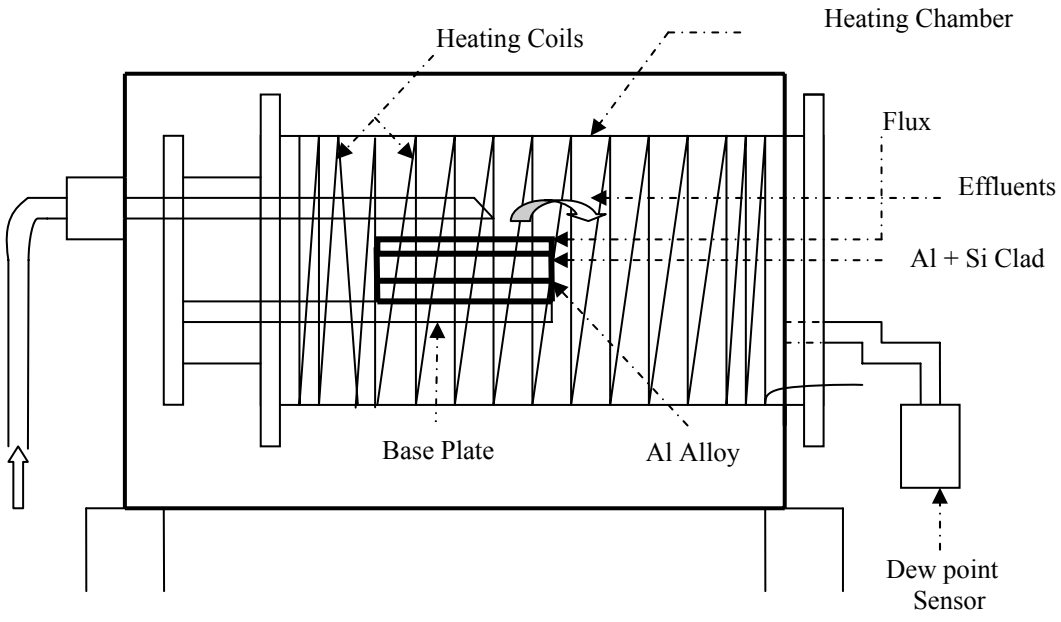

Fig. 6 Schematic Representation of the Laboratory Experimental Setup

The sample is heated by the Joule heating coils wind around the inner, transparent quartz tube of the hot zone chamber through the electrical heating mechanism. The nitrogen gas is stored in the separate tank and its flow into the chamber is monitored through the controls provided on the control board of the computer of the CAB equipment. The brazing sheet of the sample is made up of three layers; the Aluminum alloy substrate (AA 3003) over which the Aluminum + Silicon clad is laid. The layer of flux coating is added as described over the surface area. When heated, the vapors and other gases come out of the sample due to various reaction mechanisms. These effluents are carried out by the N_2 gas and passed through the dew point sensor provided on the exit port of the chamber. The measured dew point temperature signals were obtained from the Hygrometer and displayed as the digital signals on the computer. The effluent gases are vented out of the laboratory through the piping system network.

The nitrogen gas has to be passed through the heating chamber for several hours to completely remove the oxygen and humidity from it. The achieved conditions are closely monitored by measuring the dew point temperature on line continuously. Generally the heating chamber is maintained at a slightly higher pressure than that of the surroundings, and is tightly air sealed. Proper care should be taken to see that there is no direct hand contact during sample and / or equipment manipulation, in particular the interior of the hot zone before the cycle execution. The sample is placed exactly in the center of the holder plate within the hot zone. There are two thermal sensors (thermocouples) present in the chamber which are used to monitor surface temperatures of the sample. They are present on either side of the vertical sheet as shown in Fig. 14. There exits a pre-placed indentation for thermocouple contact. The feedback from these sensors is directly sent to the computer during the heating/cooling process. The feedback from these two thermocouples is referred to as Work Temperature 1 and Work Temperature 2.

After placing the sample inside the hot zone, the furnace is sealed and the pressure inside is first reduced using a vacuum system. All the screws are to be tightened at the same time to see that the terminal opening circular plate is not inclined leading to a gap to let air into the chamber. The verification of the vacuum level is performed by monitoring the

chamber pressure in real time. Subsequently, the nitrogen gas was allowed to flow into the chamber at a volumetric rate of $0.28\,m^3/hr$ for about 3 to 4 hours to reach the required dew point temperature level. (Volumetric flow rate is determined at the standard conditions 1 atmosphere and 300 K).

Dew point temperature in the present context provides precise information about the amount of H_2O present in the chamber. One of the important goals is to see that the dew point temperature at the peak brazing temperature (as well as during the ramp-up heating) always stays at a value that is acceptable for proper brazing conditions. The CAB operation follows a sequence of events, namely the ramp-up heating, melting, reactive flow, isothermal dwell and rapid quench solidification, all performed under the controlled atmosphere.

The initial, intermediate and final set points for temperature conditions are defined by the help of a computer. Also, the duration of each time zone is pre-programmed. In the first zone, i.e. the ramp-up heating, the time constraint is not entered, but the implicate command "go as fast as possible" is given. Alternatively, the ramp-rate can be adjusted by specifying longer period of time for heating. Without the time constraint generally it takes around 10 minutes to travel from 27^0C to 575^0C. The dwell time at the peak temperature is maintained for 2 to 3 minutes, depending on the size of the sample and composition and it is precisely specified. The rapid quench with industrial grade nitrogen takes place subsequently. Each test is marked by a unique description number. Data related to all tests are stored on a CD attached to this thesis.

3.4 Flux Behavior and Effluents History

It is very important to understand all the transformations that occur in the chemical states of the flux compounds and their participation in the joining process. The flux that is considered in this case is Nocolok® flux, a mixture of potassium-fluoro-aluminates. One of these compounds has physically attached water molecules (refer to Eq. (1)). During the

initial heating stages, i.e. around 80^0C, the chemically attached water molecules start being separated from the compound. Furthermore, from 80^0C to 350^0C, the progressive release of chemically bound moisture takes place [2].

Potassium-Fluoro-Aluminate in the flux gets vaporized around 400-530^0C and results in the formation of potassium aluminum fluorides.

$$2K_2AlF_5 \bullet H_2O \rightarrow KAlF_4 + K_3AlF_6 + \boxed{H_2O} \quad (3)$$

Quality Deterioration Effluent

After this phase, with the continuation of heating, from 500 - 605^0C the products from the reaction interact with the water vapors present in the chamber and results in the formation of hydrogen fluoride and alumina.

$$3KAlF_4 + 3H_2O \rightarrow K_3AlF_6 + Al_2O_3 + \boxed{6HF} \quad (4)$$

Harmful Effluent

This results in the formation of both alumina and hydrogen fluoride. Both of these products represent the sustainability concern of the process. When analyzed from the environmental sustainability point of view, HF is proven to be a toxic gas, and if taken in large amounts it results in the formation of cardiac arrests and lung cancer [15].

Alumina forms at the instant the brazing sample is exposed to air. This is because of the reactive capabilities between metal aluminum and oxygen in the atmosphere. But with the consistent and substantial amounts of moisture getting released into the hot chamber, a thick oxide layer is formed at a quick rate. This layer acts as a great hindrance as explained before to the molten aluminum filler which melts at 560-565^0C disturbing its flow towards the joint. This results in poor and inconsistent quality of joints.

So in order to stop the formation of oxide layer, either the accumulated amounts of water vapors should be driven out increasing the flow of Nitrogen gas or use fluxes which results in the lower amount of vapor release. A set of experiments is performed under

otherwise same conditions of CAB process, but using several different fluxes. The objective is to investigate vapor release rate. So based upon the dew point history and by studying the quality features of the final brazed sample, the flux influence can be uncovered.

The graphs listed in the next section represent the dew point and temperature histories for a series of tests performed by using different fluxes. These tests were performed as blind tests and the flux identity was established later. Each flux in principle has different composition which may result in varying amounts of vapors. The higher the dew point temperature, the more is the water vapor present in the system. A note of caution is needed. Since the study of the variety of flux samples is performed as a blind study, some of the behavior resembles identical features (identical samples). Before conducting the experiment, the chamber is baked out for a day by passing the nitrogen gas through it at $149^0 C$. During the ramp-up heating stage, one observes a sudden exponential increase in the dew point in the chamber, see Fig. 2. Rise in the dew point occurs at around 200 sec from the onset of ramp up heating. After conducting the experimentation, the joint formation quality of the parts has been studied, and related to the dew point temperature history. The findings are presented in the later chapters. It should be noted that a comprehensive study of joint quality must involve: (1) metallurgical analysis of the joint zone, (2) mechanical integrity, (3) corrosion resistance, (4) appearance, etc. In this study, only the fillet formation is considered.

3.5 Temperature History Data

The graphs of Figs. 7-13 show the temperature profiles for: (1) heater, (2) Work 1, (3) Work 2 and dew point. The locations for Work 1 and Work 2 thermocouples are marked in Fig. 14. The heating rate of the experiments was $38.7^0 C / \min$. From Fig. 2, and Figs. 7-13, we could observe that Work1 and Work 2 have distinct temperature profiles in most cases. The reason is a slightly inhomogeneous heating of the brazing sample. This happens more pronounced in the industry settings. During the peak brazing temperature, the differences could also be clearly seen in some cases. During the initial heating and

final quench stages the difference in most cases is almost negligible. As long as the radiation heating or convective heating techniques are used to heat the sample, these kinds of temperature non-uniformities are bound to happen. The accepted temperature differences are between max ± 5 K and ± 10 K at the peak brazing temperature to achieve a good product quality [52].

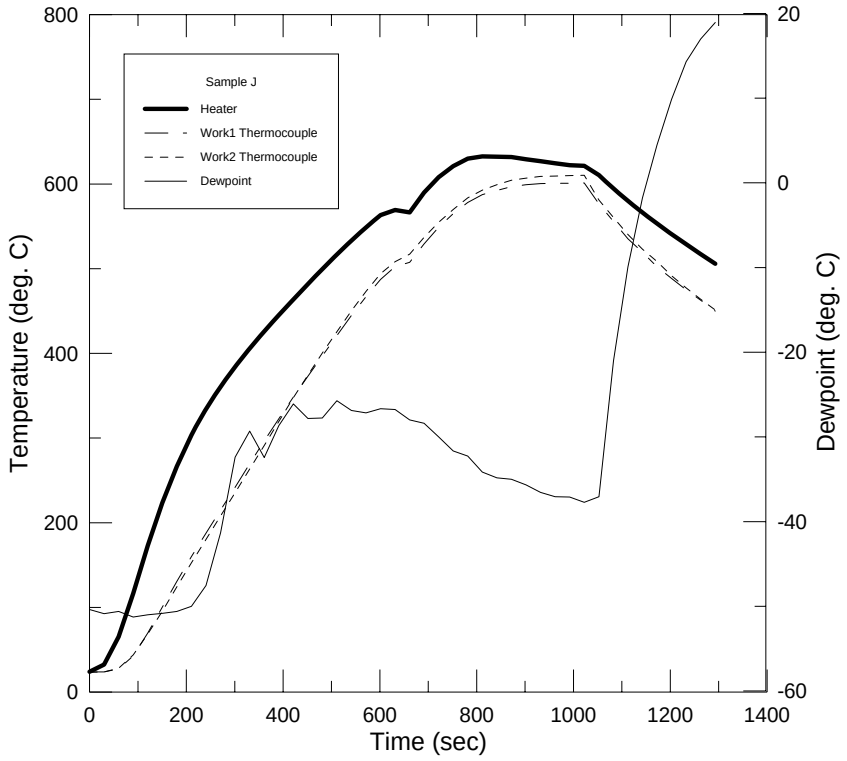

Fig. 7 Ramp-up and Dew point History of Sample J, 060105

The graph of Fig. 7 shows three different temperature profiles: the heater, the two thermocouples and also the dew point temperature history during the CAB carried out using "J" flux. The data is present in the file "SampleJ" in the CD attached to the report. The initial dew point at the onset of heating in the experiment was $-50.4\,^{0}C$. The maximum dew point recorded was $-25.7\,^{0}C$ at $421\,^{0}C$. The average dew point recorded during the dwell period was $-36.9\,^{0}C$. The increase in the dew point after 1000 sec is an artifact of experimentation and is neglected as it includes the quench sequence, see Fig. 2. The photograph of the sample obtained is presented in the Appendix E, Fig. 31. The dew point and mass flow rate magnitudes in comparison to the other fluxes are given in Eq. (3) and Eq. (4) respectively.

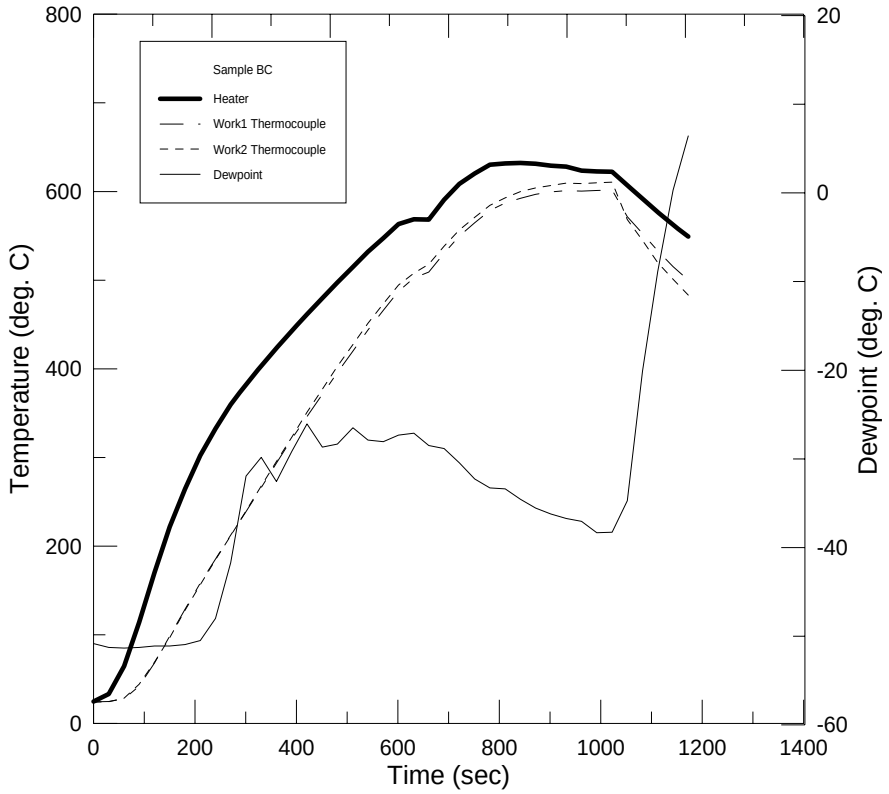

Fig. 8 Ramp-up and Dew point History of Sample BC, 060205

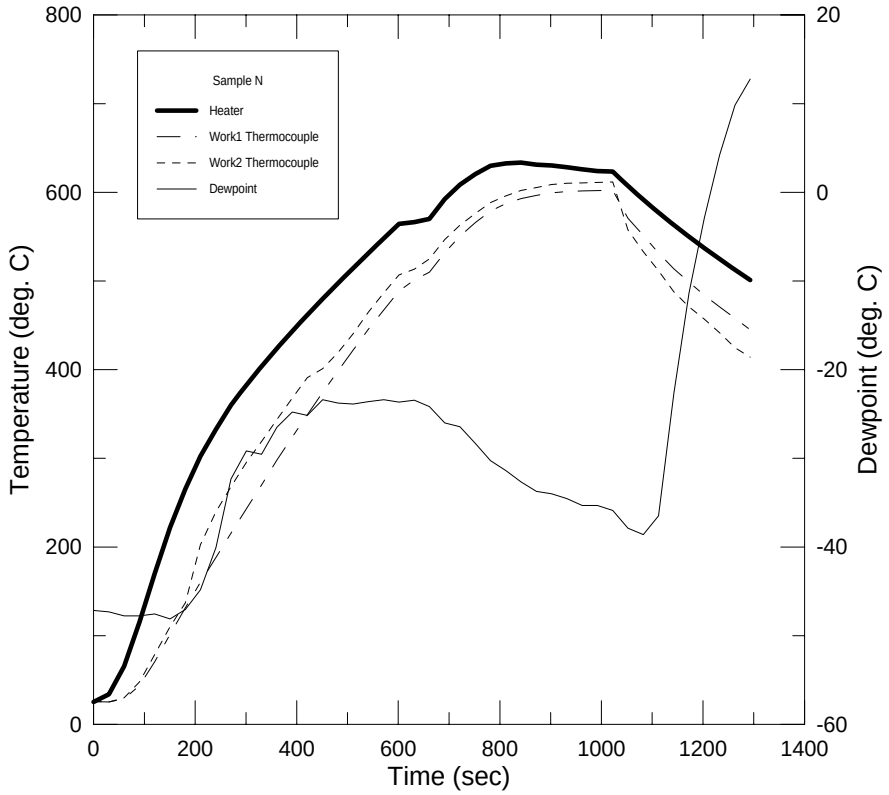

Fig. 9 Ramp-up and Dew point History of Sample N, 060305

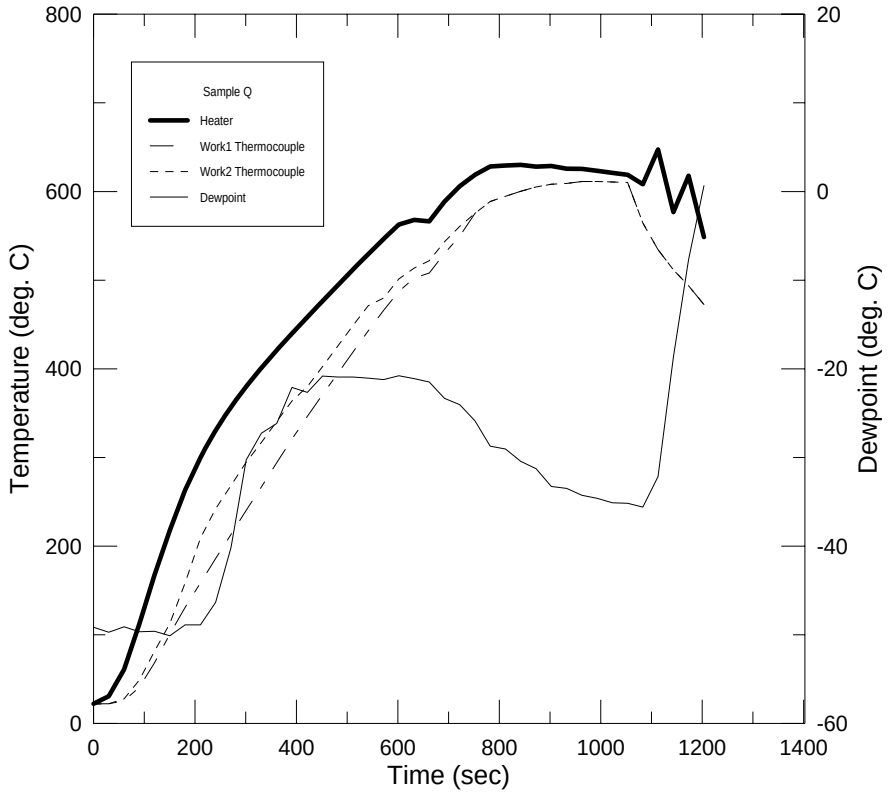

Fig. 10 Ramp-up and Dew point History of Sample Q, 061405

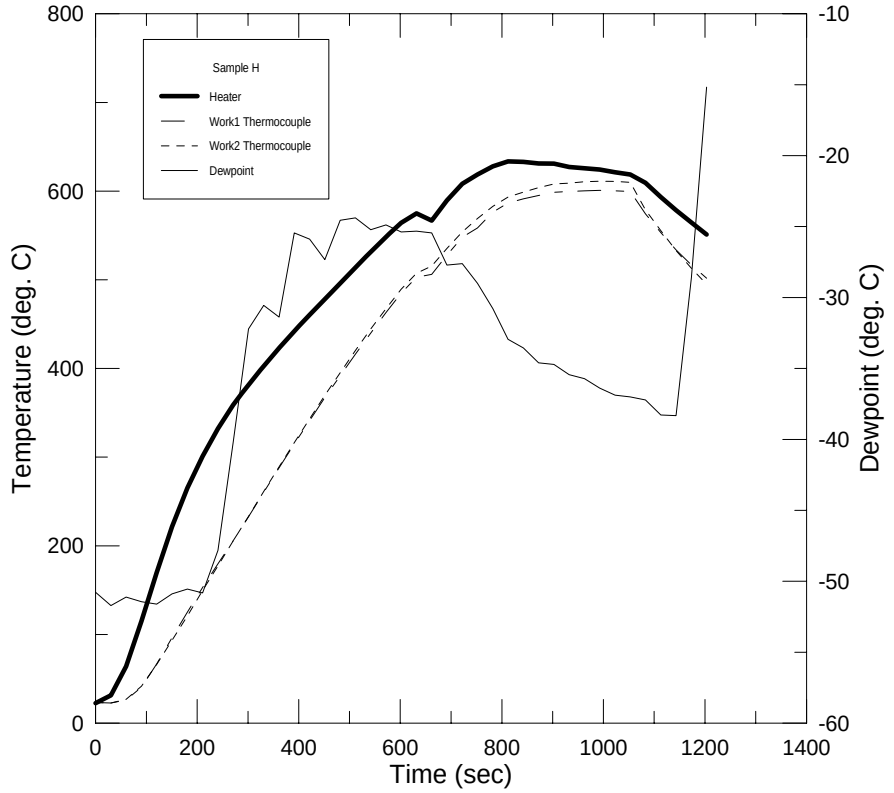

Fig. 11 Ramp-up and Dew point History of Sample H, 061505

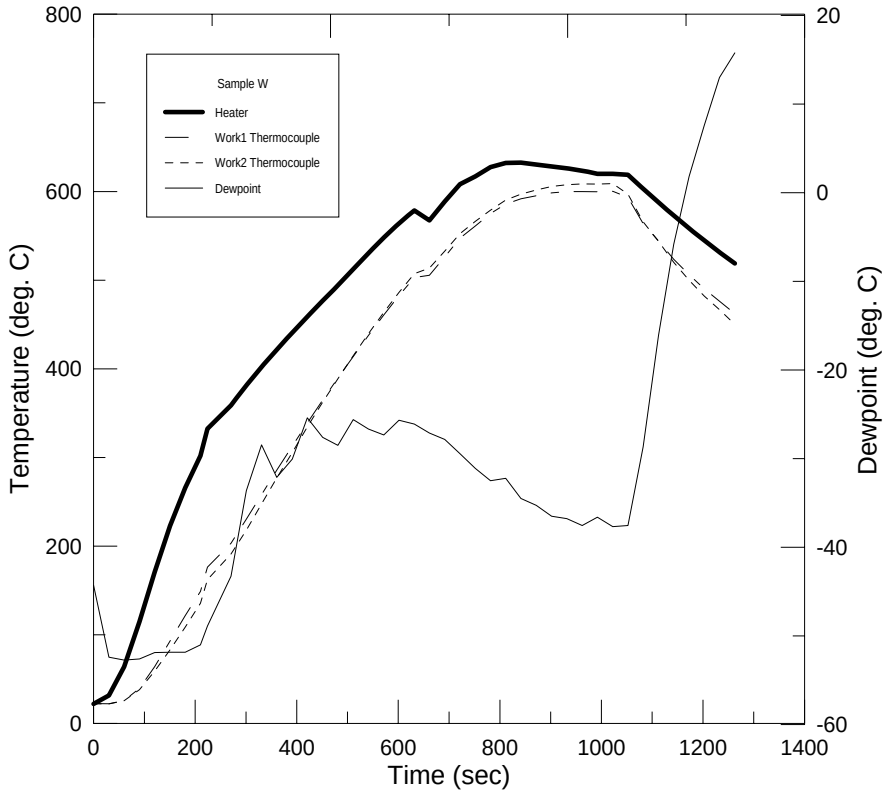

Fig. 12 Ramp-up and Dew point History of Sample W, 061605

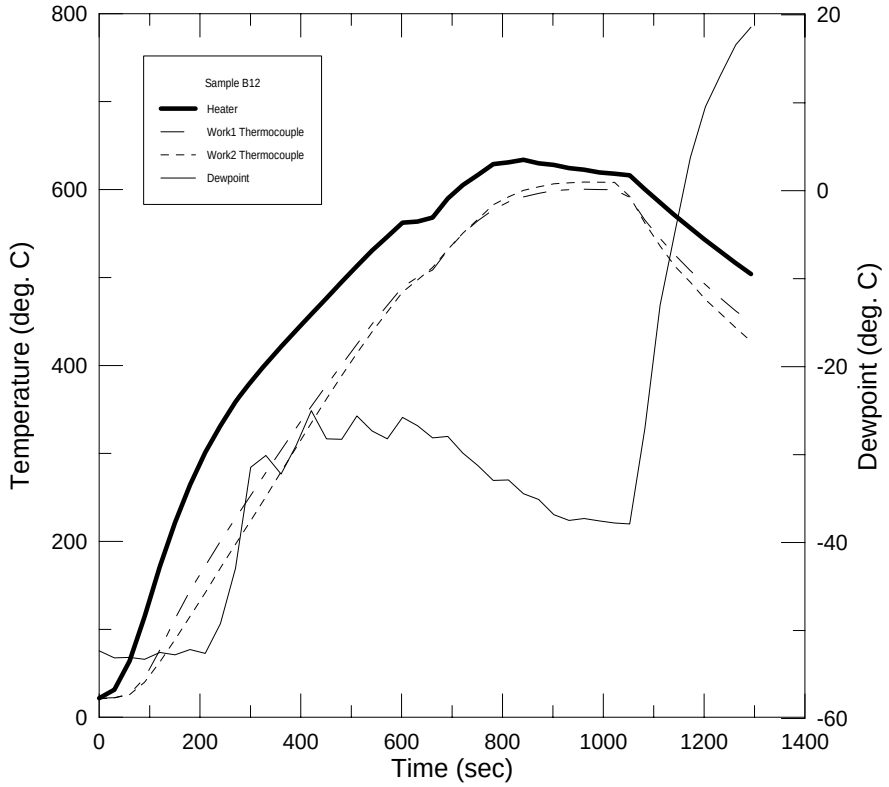

Fig. 13 Ramp-up and Dew point History of Sample B12, 061705

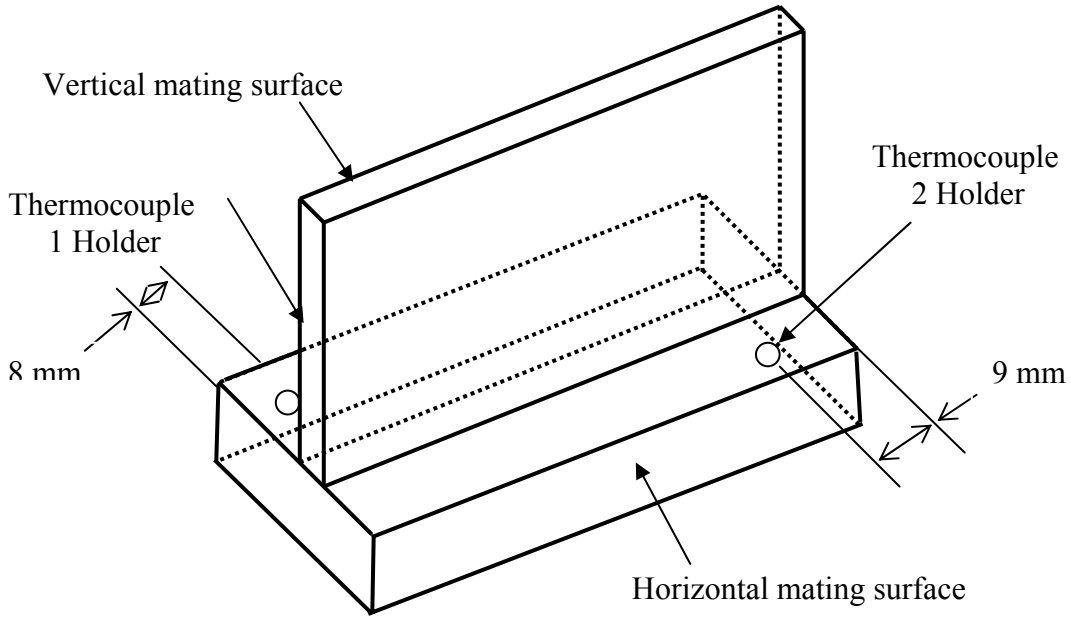

Fig. 14 3-D Representation of Sample with Thermocouple Locations

The graph of Fig. 8 shows also the three different temperature profiles: the heater, the two thermocouples and also the dew point temperature history during the CAB carried out using "BC" flux. The data is present in the file "SampleBC" in the CD attached to the report. The initial dew point of the experiment was -50.8 ^0C. The average dew point recorded during the dwell period was -37.6 ^0C. The maximum dew point recorded was -26.5 ^0C at 420 ^0C. The photograph of the sample obtained is presented in the Appendix E, Fig. 29. The dew point and mass flow rate magnitudes in comparison to the other fluxes are given in Eq. (3) and Eq. (4) respectively.

The graph of Fig. 9 shows the three different temperatures profiles: the heater, the two thermocouples and also the dew point temperature history during the CAB carried out using "N" flux. The data is present in the file "SampleN" in the CD attached to the report. The initial dew point of the experiment was -47.2 ^0C. The variation of dew point temperature at the onset of the test depends on several influential factors, of which not all were under control during testing. To mitigate this influence on the trends of H_2O

dynamics, the dew point plots were modified later to feature the same starting point. The maximum dew point recorded was -23.4 ^0C at 374.4 ^0C and the average dew point recorded during the dwell period was -35.3 ^0C. The photograph of the sample obtained is presented in the Appendix E, Fig. 32. The dew point and mass flow rate position in comparison to the other fluxes are given in Eq. (3) and Eq. (4) respectively.

The graph of Fig. 10 shows the three different temperatures profiles: the heater, the two thermocouples and also the dew point temperature history during the CAB carried out using "Q" flux. The data is present in the file "SampleQ" in the CD attached to the report. The initial dew point of the experiment was -49.2 ^0C. The average dew point recorded during the dwell period was -34.4 ^0C. The maximum dew point was -20.8 ^0C at 487 ^0C. The photograph of the sample obtained is presented in the Appendix E, Fig. 33. The dew point and mass flow rate position in comparison to the other fluxes are given in Eq. (3) and Eq. (4) respectively.

The graph of Fig. 11 shows the three different temperatures profiles: the heater, the two thermocouples and also the dew point temperature history during the CAB carried out using "H" flux. The data is present in the file "SampleH" in the CD attached to the report. The initial dew point of the experiment was -50.8 ^0C. The average dew point recorded during the dwell period was -36.1 ^0C. The maximum dew point recorded was -24.4 ^0C at 416 ^0C. The photograph of the sample obtained is presented in the Appendix E, Fig. 30. The dew point and mass flow rate position in comparison to the other fluxes are given in Eq. (3) and Eq. (4) respectively.

The graph of Fig. 12 shows the three different temperatures profiles: the heater, the two thermocouples and also the dew point temperature history during the CAB carried out using "W" flux. The data is present in the file "SampleW" in the CD attached to the report. The initial dew point of the experiment was -44.3 ^0C. The average dew point recorded during the dwell period was -37.2 ^0C. The maximum dew point recorded was -25.6 ^0C at 413 ^0C. The photograph of the sample obtained is presented in the Appendix

E, Fig. 35. The dew point and mass flow rate position in comparison to the other fluxes are given in Eq. (3) and Eq. (4) respectively.

The graph in Fig. 13 shows the three different temperatures profiles: the heater, the two thermocouples and also the dew point temperature history during the CAB carried out using "B12" flux. The data is present in the file "SampleB12" in the CD attached to the report. The initial dew point of the experiment was $-52.3\,^{0}C$. The average dew point recorded during the dwell period was $-37.5\,^{0}C$. The maximum dew point recorded was $-25.6\,^{0}C$ at $424\,^{0}C$. The photograph of the sample obtained is presented in the Appendix E, Fig. 28. The dew point and mass flow rate position in comparison to the other fluxes are given in Eq. (3) and Eq. (4) respectively.

The graph in Fig. 2 presented earlier, shows the same three different temperatures profiles: the heater, the two thermocouples and also the dew point temperature history during the CAB carried out using "S" flux. The data is present in the file "SampleS" in the CD attached to the report. Also the dew point temperature has been plotted. The initial dew point of the experiment was $-48.1\,^{0}C$. The average dew point recorded during the dwell period was $-34.7\,^{0}C$. The maximum dew point recorded was $-22.4\,^{0}C$ at $398\,^{0}C$. The photograph of the sample obtained is presented in the Appendix E, Fig. 34. The dew point and mass flow rate position in comparison to the other fluxes are given in Eq. (3) and Eq. (4) respectively.

The graphs presented in Figs. 15-17 compare the water vapor release *trends* for all the tests. The dew point history is plotted against the time. To properly identify the trends, each individual plot of a dew point temperature taken from Figs. 2 and 7-14 was re-calculated as the difference of a given value at an instant of time and the value of H_2O dew point at the initial time. This scaling forces all plots to start at the dew point difference equal to zero. At around 200 sec, there is a steep increase in the release of vapors for all tests. The release of molecularly attached H_2O must take place in the range of the sharp increase noticed. The trend clearly confirms the expectation.

Between 125 and $350^0 C$, the chemically bonded water molecules get released. So the effect is clearly identifiable in the graphs with that steep increase. Figure 15 offers the graph for the dew point histories of samples S, B12 and J against the time. The commercial flux used in the industry is "S". The performance of the other fluxes was analyzed against the performance of the standard flux. From the graph of Fig. 15, it can be clearly observed that B12 features the highest emissions and sample J has lowest emissions.

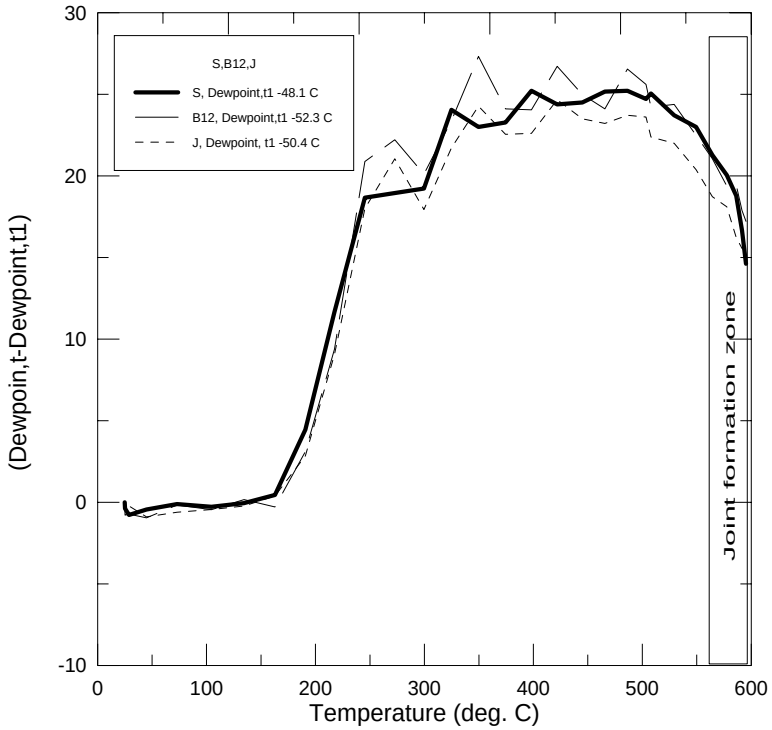

Fig. 15 Dew point Histories of Samples S, B12, J

The graph of Fig. 16 compares the dew point histories of samples BC, N again with that of sample S. The emissions in the case of S are the highest in this case. The emissions in the case of BC are lower than that of N. Finally, it is clear from the graph of Fig. 17 that the sample Q has the highest amount of vapor release and sample W has the lowest amounts of vapor release. The graphs in Figs. 15-17 have been plotted from the files 1-9 included in the CD.

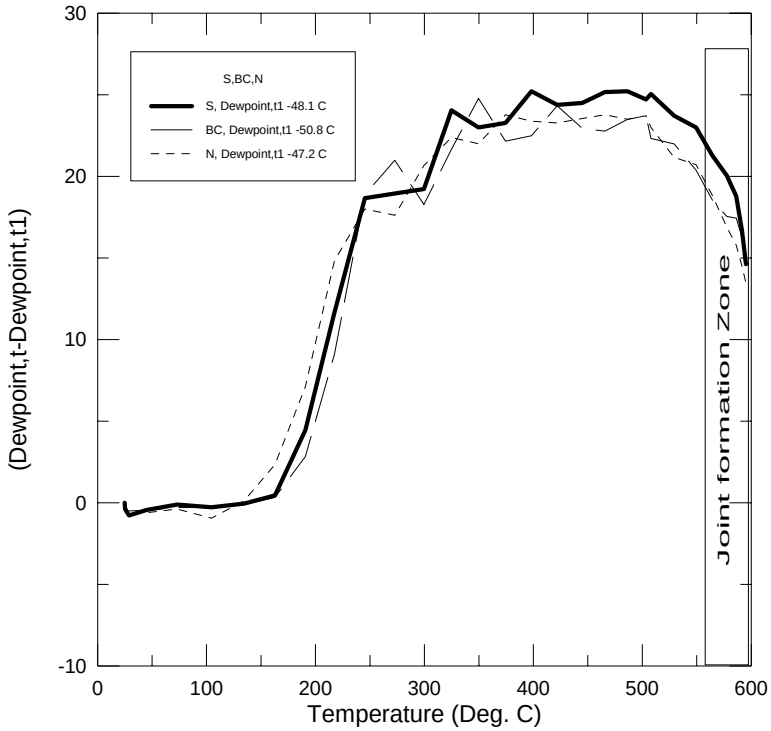

Fig. 16 Dew point Histories of Samples S, BC, N

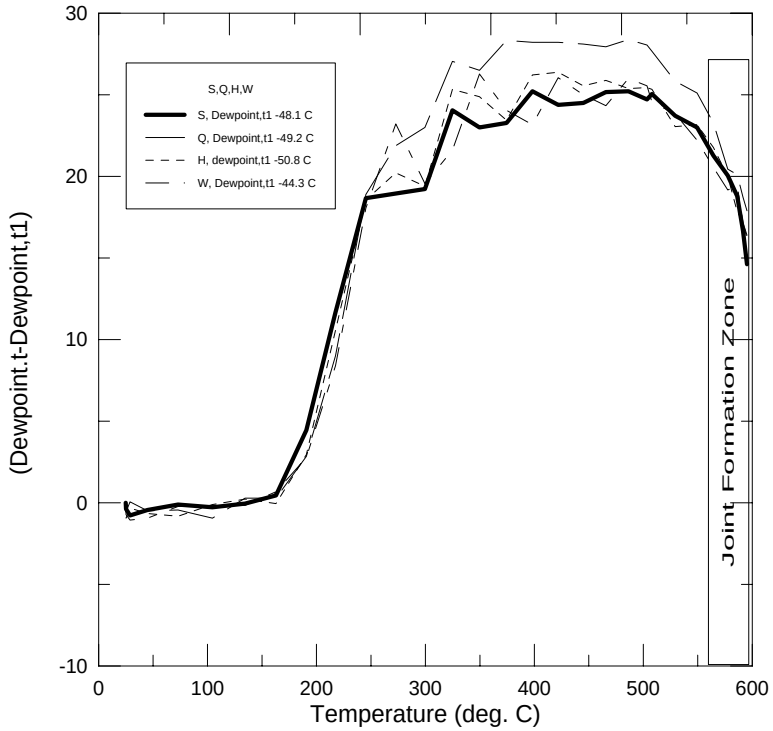

Fig. 17 Dew point Histories of Samples S, Q, H, W

3.6 Quality Inferences

In this section, the comparisons will be made between absolute emission quantities for effluents related to different tests and the measure of joint formation. This measure is the length of the joint fillet; see Fig. 4 and Fig. 18. All the dew point histories are plotted against time in Fig. 19. The mass flow rates of the vapor release are calculated from the dew point history of each test and presented in Fig. 20. The calculation of mass flow rates is discussed in section 4.3 (see also Appendix C). In Table 1 the fillet lengths are summarized next to an indication of humidity presence, in Figs. 7-13.

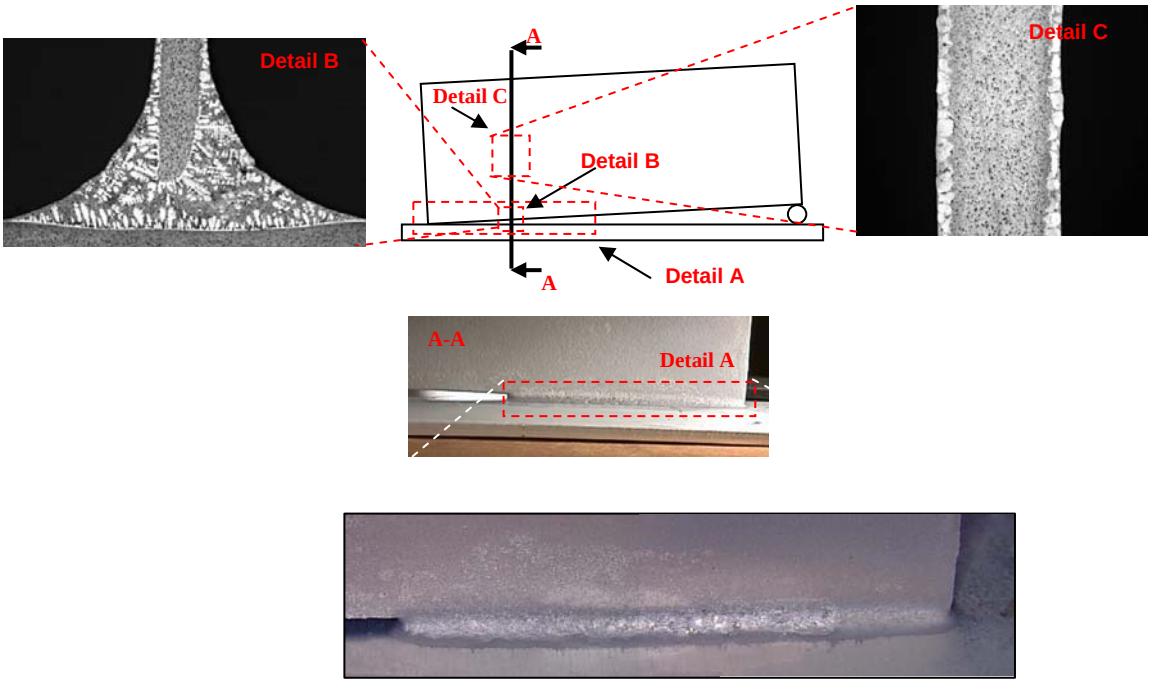

Fig. 18 Cross Section of the Vertical Plate and the Length of Fillet

The sample is cut into half vertically at section A-A as shown in the figure. This is done to study the clad metal flow. The top left side view actually is used to study the fillet cross section. This analysis is beyond the scope of the thesis.

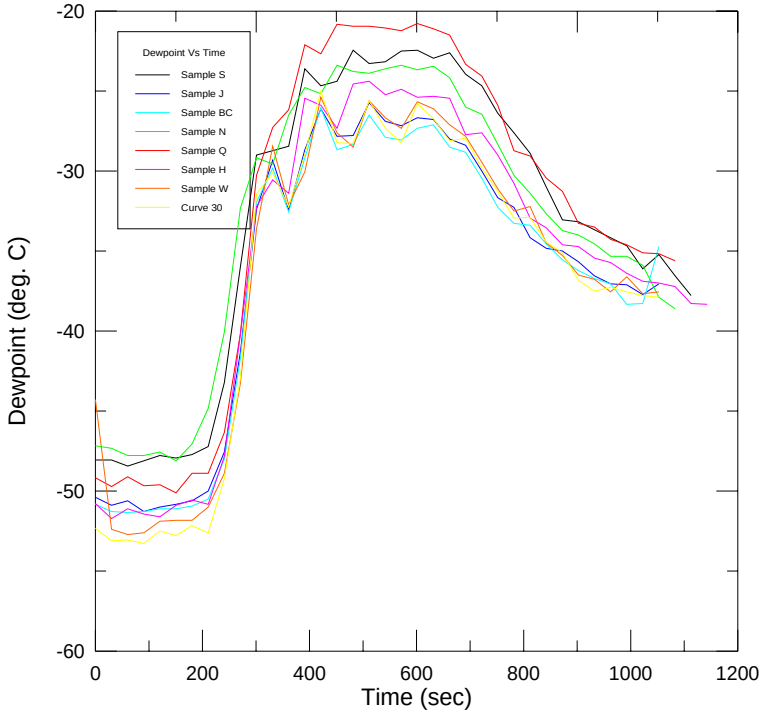

Fig. 19 Dew point Histories of All Samples

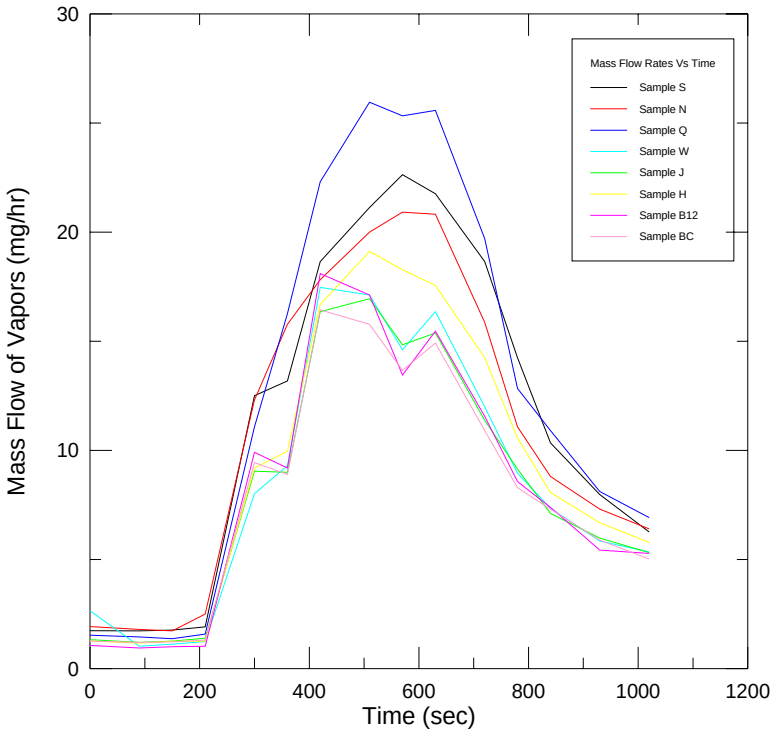

Fig. 20 Mass Flow Rates of vapors for All Samples

Table 1: Length of Fillet Joints

Sample	Length of fillet (mm)	Dew point in clad Melt zone ^0C	Average dew point in dwell (^0C)
S	28.3	-27.6	-34.7
H	27.4	-30.8	-36.1
W	25.6	-32.5	-37.2
N	28.8	-30.3	-35.3
B12	28	-33	-37.5
J	26.7	-32.3	-36.9
Q	27.8	-25.9	-34.4
BC	29.7	-33.3	-37.6

It can be observed from the Table 1 that the length of the fillets measured for all the samples were relatively close to each other. This is the case, in particular when the dew points in the melt zone of the clad were also close to each other. This means that identical conditions (i.e., similar amount of mass flow rates of water vapors) were present in the chamber when the liquid filler metal flows towards the joint. The formation of equal amounts of oxide layers presented similar resistance to the flow in each case and resulted in the similar joint formations. Note, for example, the case BC is characterized with the best fillet formation, hence one may expect to see the dew point both in the melt zone and during the dwell period to be the lowest. This is exactly the case, see Table 1. In the series of tests conducted, the dew point histories are close to each other and the filler length should be close to each other as well. The average dew point of the dwell zone showed relatively small deviation from each other. It is known that at the peak brazing temperatures, the tendency of the flux compounds reacting with the oxide layers is pronounced what creates an impact on the filler metal flow [1]. The uncertainty of the length measurement is around 0.05 mm.

Analyzing the above data, it can be understood that almost similar conditions were present at the crucial stages of joint formation (clad melt and joint formation at peak stages) in all the cases. The reason being that some of the fluxes used in the experiments were the derivatives of a standard flux i.e. some of them contained the same proportions of the constituents and similar compounds. The small variations in the above lengths could be attributed to minor factors like the variation in the joint clearances, the spread of the flux etc. From this experimentation it has been learnt that the exponential increase of dew point (also MFR, see Fig. 19 and Fig. 20) starts at around $80^0 C$ and sharp increase can be noted at $177^0 C$. Literature [1] [4] refers to the same temperature limit as the starting point of dissociation reaction. Therefore, one can infer that the main and primary source of the vapors is the flux itself. More experimentation has been performed and presented in Chapter V to analyze the influence of heating rates on the dew point conditions during the peak stages of joint formation.

CHAPTER IV

MODEL PREDICTIONS

Although it is quite well known that the possible reason for the release of vapors (leakages residue and the water inflow neglected) is the flux itself, this exercise is intended to illustrate whether a very simple way of analyzing and interpreting the data from the CAB laboratory experimentation is possible. Data from an independent TGA analysis were corroborated to make this modeling. The quantification of the H_2O vapor emissions based on the model was done for each test case, and all the results were compared with each other. Through this comparison we expected to find that during the period where there is exponential increase in dew point temperature in CAB experimentation, there is also a complementary rate of increase in the vapor release from the flux in the TGA experimentation.

4.1 Modeling Approach

System

The system we are considering is the gas mixture (Nitrogen + effluents) in the furnace chamber in which the sample to be brazed is kept. The chamber is being supplied with the high purity nitrogen gas during brazing cycle. This is a typical open thermodynamic system with a steady flow of nitrogen and additional release of effluents.

Assumptions

- The flow of the background gas (nitrogen) is in the steady state.
- The source of water vapors getting released out during the process is considered to be generated by the dissociation reaction of the flux exposed to heating [1].

- The dissociation is considered to be analogous to a simple reaction of the first order.
- The pressure inside the chamber is considered to be constant and close to the atmospheric pressure.

The rate of the reaction is assumed to obey the relationship $r_{(H_2O)} = [kC_{H_2O,0}e^{kt}]$. The exponential factor in the rate of reaction should signify an exponential increase of the dew point temperatures (or the increase of the mass flow rate of the effluents) during the process, and also should be consistent with the mass loss of flux in the TGA analysis which is to be performed independently. The first order reaction is assumed to be the one during which the rate of reaction is directly dependent upon the concentration of the reactant.

One condition to be satisfied in order to prove that the dissociation reaction is of the first order is that the logarithm value of the mass flow rates of vapors vs. the temperature (or time) should obey a linear dependence [56] [55]. A typical graph plotted between $\ln(\dot{m})$ and time 't' for a second order and first order reactions looks like sketched in Fig. 21a and Fig. 21b respectively. In the next section, the graphs (see Figs. 22, 23, and 24) between logarithmic values of the mass flow rates of water vapor and time obtained from the TGA data of samples S, H and W are plotted. Comparison between these results was made to support the assumption of linearity.

4.2 Thermogravimetric Analysis (TGA)

Thermogravimetric analysis (TGA) is an analytical technique which is used to determine a material's thermal stability and its fraction of volatile compounds by monitoring the change in weight with respect to change in temperature [61] [64]. The tests are generally carried out in air or in the inert gas (Helium or Argon) atmospheres. In addition to the weight changes, the temperature difference between the specimen and one of the reference pans (Differential Thermal Analysis, DTA) are carried on. This technique is

used to monitor the energy released or absorbed due to chemical reactions during the heating process. A TGA plot is presented in Fig. 3.

To be able to independently verify the validity of the analysis performed on the set of data obtained from the CAB tests in continuous brazing furnace, the set of TGA data obtained for a flux from the considered set of fluxes is analyzed to establish mass reduction during heating (to be proportional to effluents) [11]. The simple analysis given below presents the methodology in which the weight loss of the Nocolok flux during the Thermogravimetric analysis tests has been converted into the mass gain of water vapors as effluents. The reaction constant k is calculated as shown in the following section. The dissociation reaction is given by Eq. (2).

4.2.1 Rate of reaction

The rate of reaction is assumed to be represented by the amount of water vapor (mass units or units of the quantity of matter i.e., moles) that is released per unit volume per unit time. The rate of reaction in the case of a first order reaction is defined as [56]

$$r_{(H_2O)} = \frac{dC_{H_2O}}{dt} \tag{5}$$

We assume that the rate of change of the concentration is directly proportional to the concentration

$$\frac{dC_{H_2O}}{dt} \propto C_{H_2O} \tag{6}$$

Now assuming a linear relationship involving a reaction constant 'k', we get

$$\frac{dC_{H_2O}}{dt} = kC_{H_2O} \tag{7}$$

or,

$$\frac{1}{C_{H_2O}} dC_{H_2O} = kdt \tag{8}$$

Integrating both sides, one gets formally

$$\int_{C_{H_2O,0}}^{C_{H_2O}} \frac{1}{C_{H_2O}} dC_{H_2O} = \int_0^t k\, dt \tag{9}$$

After integration, we have

$$\ln\left(\frac{C_{H_2O}}{C_{H_2O,0}}\right) = kt \tag{10}$$

$$C_{H_2O} = C_{H_2O,0} e^{kt} \tag{11}$$

Where, k is the reaction constant, C_{H_2O} is the instantaneous mass concentration of water vapor in the considered volume, $C_{H_2O,_0}$ is the initial mass concentration of water vapor in the control volume. The mass concentration can be defined as the ratio of the mass flow rate of the water vapors to the volumetric flow of the N_2 gas mixture (N_2 and water vapors).

$$C_{H2O} = \frac{\dot{m}_{H_2O}}{\dot{V}_g} \tag{12}$$

$$C_{H2O,0} = \frac{\dot{m}_{H_2O,0}}{\dot{V}_{g,0}} \tag{13}$$

Expressing equation (10) in terms of mass flow rates and volumetric flow rates, we get

$$\frac{\dot{m}_{H_2O}}{\dot{V}_g} = \frac{\dot{m}_{H_2O,0}}{\dot{V}_{g,0}} e^{kt} \tag{14}$$

Where, $\dot{m}_{H_2O}$ and $\dot{m}_{H_2O,0}$ are the mass flow rate of an instant of the time and initial mass flow rate of the water vapor in, say TGA chamber respectively, whereas $\dot{V}_g$ and $\dot{V}_{g,0}$ are the instantaneous and the initial volumetric flow rates of the gas mixture. Compared to the large inflow of the N_2 gas, the water vapors generated during the test are small. So, there will not be a considerable difference between the initial and instantaneous volumetric flow rates of the gas mixture and both can be treated as almost identical. The Eq. (14) now becomes

$$\dot{m}_{H_2O} = \dot{m}_{H_2O,0} e^{kt} \tag{15}$$

In Thermogravimetric (TGA) analysis, the mass loss with respect to time and temperature is monitored during heating. From these values, the mass flow of moisture in the furnace

can be predicted. The difference between the initial mass of the sample and the mass at any time gives the mass that has been evaporated per unit time until that point. But the evaporated mass may not necessarily be the water vapor. As we know the flux under examination is the Nocolok® flux, which has the simplified composition of $K_2AlF_5 \bullet H_2O + KAlF_4$. Let us assume that the flux has 15 % of $K_2AlF_5 \bullet H_2O$ and 85 % of $KAlF_4$. If W_{in} is the initial weight of the sample and W_t is the instantaneous weight at an instant time point't', then [0.15 (W_{in} - W_t)] is the mass of water vapor that is evaporated.

$$\dot{m}_{H_2O} = 0.15(W_{in} - W_t) \tag{16}$$

W_{in} is the initial weight of sample, say (for a selected test) W_{in} = 9.4113 gm (from TGA data) [11]. W_t is the instantaneous weight of the sample.

The reaction constant can be calculated by plotting the graph between $\ln(\dot{m}_{H_2O})$ and the time't'. The slope of the curve (assumed to be linear in that coordinate system) gives the value of k. If a single line can be fitted through the experimental data, k would be constant, otherwise the slopes of different line segments would be variable.

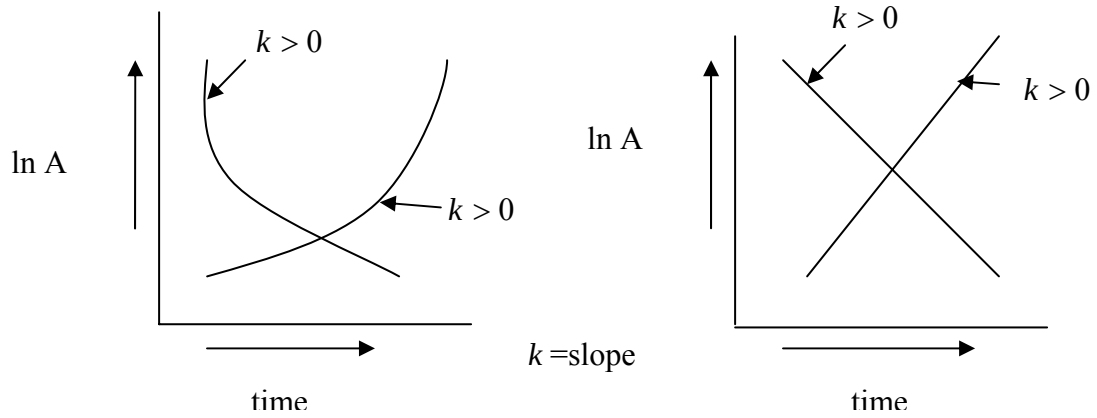

Fig. a Second order reaction

Fig. b First order reaction

Fig. 21 ln A Vs time profiles for first order and second order reaction constants

The graphs shown in Fig. 21 are showing the generalized trends of concentration decrease on ln A vs. time plot for first order and second order reactions. In our study, an increase in the mass flow rates of effluents takes place as the time progresses and so the positive slope should be expected. The Fig. 21a resembles a parabolic profile, whereas Fig. 21b indicates linear profiles.

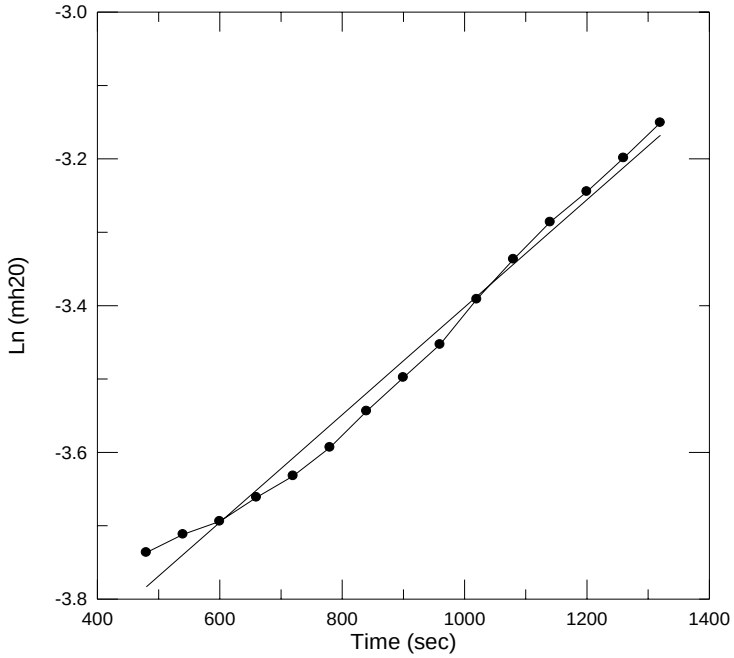

Fig. 22 Logarithm of Mass Flow Rates fitted against time from TGA S Test

Fig. 22 presents the graph of the logarithmic values of mass flow of water vapor against time. This is plotted from the TGA data to calculate k (slope) value. The data for the graph have been presented in the appendix B. This graph resembles Fig. 21(i). The spline passing through all the points presents the actual experimental data, and the straight line that passes through the points is a curve fitted with the slope of 0.000734 sec^{-1} for $480 \leq t \leq 1320$ sec. The data supports an assumption of dissociation being of the first order. Similar linear trend could be observed for other samples, W and H, Fig. 23 and Fig. 24. The k value is calculated for each case. All the buoyancy effects (an artifact of the experimental procedure) (see Fig. 3) have been not considered and the reaction

constant is calculated in between the time instants at 480 sec (8 min) and 1320 sec (22 min). The graphs in the Figs. 22-24 are plotted from the data contained in the 'k-value' file included in the CD.

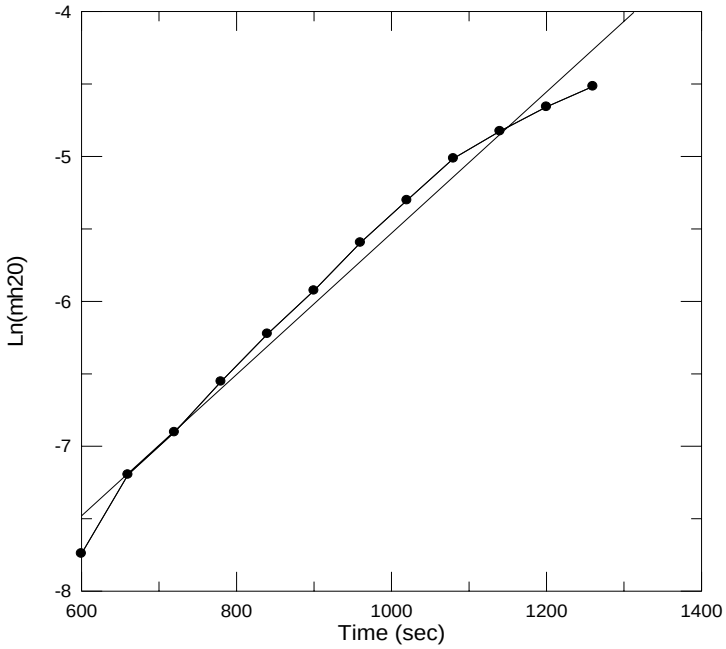

Fig. 23 Logarithm of the mass flow rates fitted against time from TGA W Test

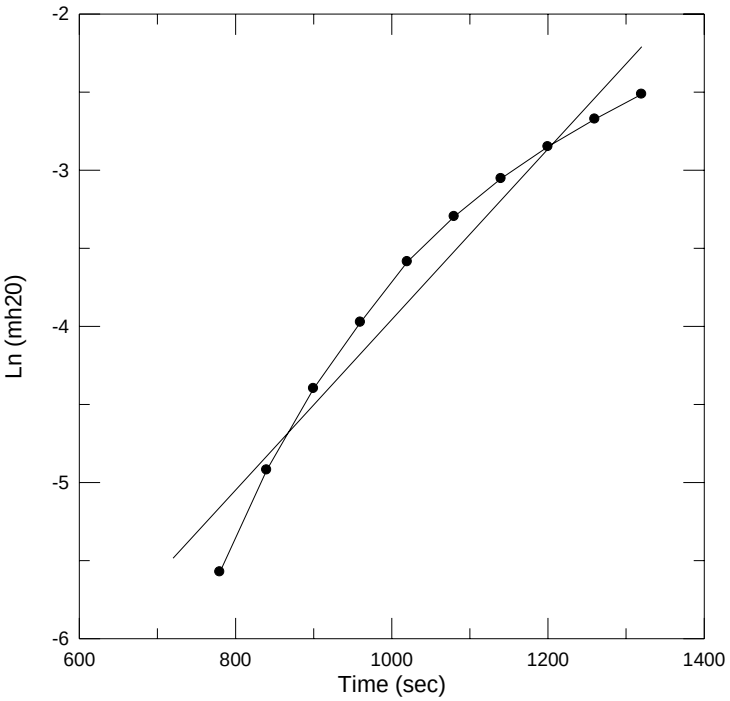

Fig. 24 Logarithm of the mass flow rates fitted against time from TGA W Test

From the reaction constant calculated as shown above, the mass flow of water vapors in the CAB furnace can be predicted by using the Eq. 15. The input data are as follows
Initial volumetric mass concentration of water vapor in CAB furnace, $\dot{m}_{H_2O,0}$

$$\dot{m}_{H_2O,0} = 1.24698 \times 10^{-6}\, kg/m^3$$

Reaction constant, k (from TGA-S data) = $0.000734\ \text{sec}^{-1}$ Instantaneous time in CAB process, t (sec)

The predicted values of mass flow rates of water vapors from the k value which is calculated from TGA data are presented in appendix D. $m_{H_2O,0}$ is calculated from the initial dew point temperature ($-48.1\,^0C$) (Sample S file attached in CD) by using the equations from (17) to (24). In the Section 4.3, the methodology of the quantification of the H_2O effluents from the dew point readings of laboratory CAB furnace tests is presented.

4.3 CAB Furnace Experimental Data

If one relates the specific humidity within the chamber to the dew point temperature, the mass flow rate of water vapor can be calculated knowing the mass flow rate of nitrogen. Specific humidity within the chamber is defined as the ratio of the mass of water vapor to the mass of gas phase (Nitrogen in this case). This specific humidity when multiplied by the mass flow rate of nitrogen will give the mass flow rate of water vapor present in it.

$$\psi = \frac{\dot{m}_{H_2O}}{\dot{m}_{N_2}} \tag{17}$$

From Eq. 16 one gets,

$$\dot{m}_{H_2O} = \psi\, \dot{m}_{N_2} \tag{18}$$

Where,

$$\dot{m}_{N_2} = \rho_{N_2} \dot{V}_g \tag{19}$$

Also we know that [41], $$\psi = \frac{M_{H_2O}}{M_{N_2}} \frac{p_v}{P - p_v} \tag{20}$$

$$\psi = \frac{18}{28}\frac{p_v}{P - p_v} \tag{21}$$

$$\psi = 0.6429\frac{p_v}{P - p_v} \tag{22}$$

Where [24],

$$p_v = 610.78e^{\frac{17.294T_d}{T_d + 265.5}} \tag{23}$$

In Eq. (22), the relevant variables are as follows.

T_d = Dew point Temperature ^0C

p_v = Partial Vapor Pressure (N/m^2)

P = Pressure inside the chamber (N/m^2) [1 atmosphere = 101325 (N/m^2)] [14]

ρ_{N_2} = Density of Nitrogen (kg/m^3) [1.2506 (kg/m^3)] [14]

$\dot{V}_g$ =Volumetric flow rate of N_2 gas mixture [0.0238 $(m^3/\sec)$]

The specific humidity is calculated using the partial pressures of the water vapor filled with moist nitrogen within the chamber. Since we have the dewpoint temperature data, we use Eq. 23 to find the partial pressures of H_2O vapors in the mixture. From Eq. 15, the mass flow rate of water vapor can be found out by multiplying the specific humidity with the mass flow rate of nitrogen at given standard conditions. The mass flow rate of nitrogen is calculated as the product of the density and volumetric flow rate of nitrogen. Therefore the mass flow rate of nitrogen from Eq. 14 is ($\rho_{N_2}\dot{V}_g$). The mass flow rate of moisture at any given temperature T is found by the following equation:

$$\dot{m}_{H_2O} = \psi\rho_{N_2}\dot{V}_g$$

$$\dot{m}_{H_2O} = 0.6429\rho_{N_2}\dot{V}_g \frac{610.78e^{\frac{17.294T_d}{T_d + 265.5}}}{P - 610.78e^{\frac{17.294T_d}{T_d + 265.5}}} \quad kg/\sec \tag{24}$$

4.4 Comparison of Mass Flow Rate Trends

The mass flow rates of the vapors calculated from the dew point temperature values, and from the model prediction are presented in Appendix D. Fig. 25 shows the trends of increase in both of these cases for all the three fluxes S, H, W. From the graph in Fig. 25, we can conclude that for sample W, the values of the mass flow rate in the model and the experimental cases are close to each other until 400 sec and vary after that considerably. The model predictions beyond this zone still increase at an exponential rate whereas the values in the experimental case see a downward trend. The same trend could be observed in the case of sample H. In the case of S, the experimental values are higher than that of the model predictions because of the extreme lower k values from its TGA data.

It is hypothesized that this is because of the influence of additional factors of the system on moisture levels. Namely, the adopted model is very simple and does not include many possible influences. For example the Nitrogen gas passing through the chamber drives off all the accumulated vapors in the CAB furnace as an open steady state system. The heating rates used in the CAB experimentation could also influence vapor emissions, and may result in lower dew point levels (refer to Chapter 5). No such factors have been taken into consideration for the model predictions. A more sophisticated model which could take into consideration the factors that influence mechanics of vapor release, and other external factors (N_2 gas and mass flow rates) that control the dew point levels in CAB furnace is not within the scope of this Master's thesis.

The research by Claesson [13] developed an online computer system that could be attached to the brazing furnace and monitor the oxygen levels. Presence of higher amounts of oxygen would prompt additional nitrogen gas to be supplied. Corresponding transient model would include more factors that may influence the moisture levels. The graph in the Fig. 25 has been plotted from the data contained in the COMPME-S, COMPME-W, and COMPME-H files included in the CD.

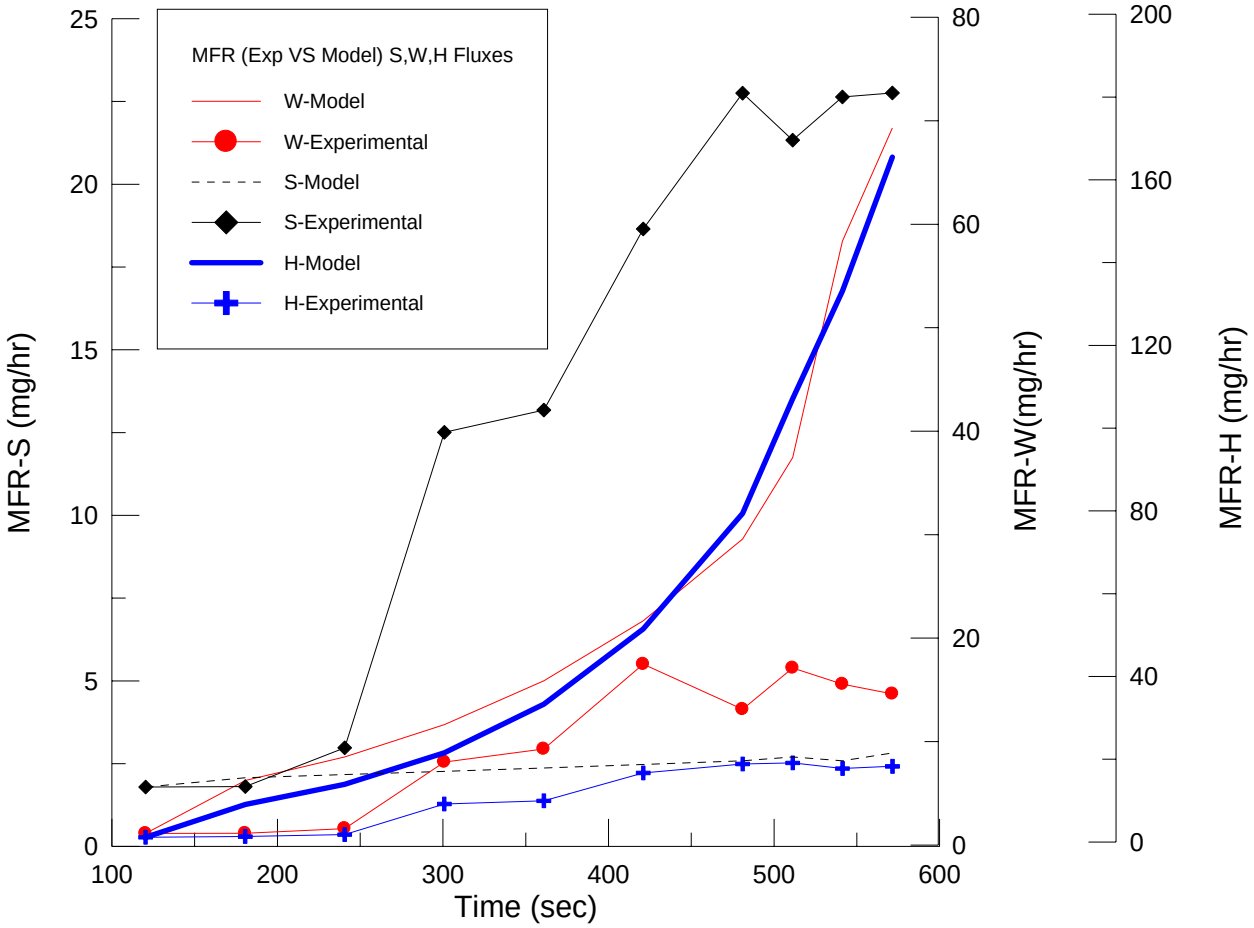

Fig. 25 Model vs. Experimental

CHAPTER V

INFLUENCE OF RAMP-RATES ON WATER VAPOR RELEASE

5.1 Background

Our analysis presented so far has taken into account only one influential parameter – humidity level – that may influence joint quality. This very simplified scenario does not include other phenomena on the interface between molten clad and substrate. Namely, while one may speculate that a prolonged ramp-up heating may reduce humidity (hence positively influence product quality) at the same time, this would separately influence joint formation due to simultaneous influences of the time of exposure of molten liquid and substrate to elevated temperatures. In this chapter, we intend to show how such possibly opposing factors may lead to more complex outcomes than expected.

Many studies have been conducted to understand the influence of ramp rates on the length of the fillet formed during the brazing process [32] [31] [6]. The ultimate aim of those studies was usually to study the silicon diffusion under varying ramp rates. It is very well known that the clad material in aluminum brazing consists of an alloy of aluminum and silicon. If more amounts of silicon diffuse into the base metal, lower amounts of clad will be available to form a joint. As a result, short brazing joints are obtained hampering the quality of the product. Also, it is known that the silicon diffuses to the substrate during the peak brazing temperatures and investigations have been performed to study this phenomenon. Research performed by Gao et al. [32] involved in the determination of the silicon diffusion coefficients prior and during the peak temperature of brazing. Terrill [33] developed a mathematical model to predict the diffusion of silicon. By computing the amount of cladding available, his model could predict the length of the fillets accurately [6]. The relation between the Si diffusion and the quality of the joint (length of the fillet in this case) has been studied thoroughly. The

research by Hui and Sekulic [31] involved varying ramp rates to develop the transient moving boundary diffusion model of silicon into the substrate and the same has been corroborated with the empirical findings.

It is very important to reduce this diffusion during brazing. Engstroem [34] analyzed a multi layered clad aluminum material which significantly reduced this Si diffusion which finally resulted in the improved brazeability and strong brazing joints. Also, it has been found that the dwell times at the peak brazing temperatures has an influence on the substrate dissolution and core metal erosion in the joint zone [35]. Besides these, the selection of the materials, the process parameters and the geometrical features of the joint decide thermal and mechanical integrities of the brazed joints [35]. Research conducted by Sekulic et al. [6] revealed that the mass flow rates of the molten clad/ filler depend heavily on the following set of parameters: (1) the silicon content in the clad and substrate composition, (2) cladding ratio, (3) ramp-up rate during the heating segment of the brazing cycle (4) peak brazing temperature and (5) flux coverage (keeping other process and material characteristics/ conditions under control).

The different ramp rates could be easily obtained by varying the time periods of heating between initial and peak temperatures in the CAB laboratory equipment. Such analysis was performed and presented next. The range of heating rates that could be imposed in the experimental equipment used is from $60^0 C/\min$ to $10^0 C/\min$. It is very important to maintain low amount of water vapors at the peak stage of the brazing process. In the longer duration of the heating periods, the Nitrogen gas flowing through the chamber has more time to remove these vapors from the system. By doing so, the conditions for the formation of good joints are improved because of the expected lower amounts of alumina formation, but at the same time other adverse factors may lead to an ultimately different result (such as Si diffusion, liquid metal penetration, erosion, etc.)

A set of calculations has also been performed to determine the volume that could be displaced by the nitrogen gas under varying heating rates. The mass flow rate of the nitrogen gas and the volume of the chamber are known. Given the ramp rates and the

peak brazing temperature, the time it requires to reach the peak process stages could be estimated. Knowing this time period and the flow rate of Nitrogen gas, the displaced volume of the chamber could be estimated. The larger this displaced volume, the more are the chances of eliminating the vapors from the chamber before reaching the peak stages. The input data used in this estimation are as follows. Radius of heating chamber, r = $0.057\,m$, Length of heating chamber, l = $0.254\,m$, Volume of chamber, v = $0.00259\,m^3$, Nitrogen in-flow, $\dot{m}_{N_2} = 0.02832\,m^3/hr$

The volume that can be displaced by the Nitrogen using different heating rates before reaching peak temperatures in the chamber is presented in Table 2. The more volume it displaces, the better it is for the process (but other adverse effects may be present). All the calculations have been presented in the appendix G.

Table 2: Displaced Volumes

Heating Rate ($^0C/\min$)	Percentage (%)
30.07	364.3
12.02	912.3
20.05	546.5
60.17	182.2

From Table 2: we can see that the ramp rate of $60.17\,(^0C/\min)$ leads to the situation in which the chamber volume is displaced at least two times before reaching the peak brazing temperature, whereas the $12.02\,(^0C/\min)$ displaces the chamber volume 9 times before reaching the peak temperatures. The slowest ramp rate is assuming the nitrogen gas to displace chamber volume many times, thus resulting in the lowest amount of water vapors during the peak segments of brazing process. The same point has been reflected in the Fig. 27 which recorded the lowest dew point among all the other ramp rates. The

20.05 (^0C/min) and 30.07 (^0C/min) leads to the gas displacement of the chamber volume 6 times and 4 times, respectively. Lower dew points are recorded in the case of lower ramp rates in Fig. 27.

The expectation that longer ramp rates may assist positively brazing may be, however, very misleading. The literature review confirmed that the lower ramp rates (higher process time) results in more silicon diffusion which results in the short fillet length formation. In order to uncover actual trade off between these influences, experimentation has been conducted with the T-joints and Nocolok® flux. Four different experiments were conducted with different ramp rates by maintaining the same process conditions in each case. The details of the experimentation are given next.

5.2 Experimental Procedure

A set of experiments performed with Nocolok® flux gave various dew point readings. The experiments were performed with the same dwell time i.e., 2 minutes at the peak brazing temperature. The clad used in the process is Al+Si alloy AA4343 and the base metal used is an aluminum alloy AA3003.

Experiment 1 (test # 030206) Experiment 2 (test # 030306)

Temperature range (^0C)	Heating rate (^oC/min)	Dwell duration (min)	Temperature range (^0C)	Heating rate (^oC/min)	Dwell duration (min)
0 to 602	30.07	-	0 to 602	20.05	-
602	-	2	602	-	2

Experiment 3 (test # 030606)			Experiment 4 (test # 030706)		
Temperature range (^0C)	Heating rate ($^oC/\min$)	Dwell duration (min)	Temperature range (^0C)	Heating rate ($^oC/\min$)	Dwell duration (min)
0 to 602	60.17	-	0 to 602	12.02	-
602	-	2	602	-	2

The different profiles of the heating rates could be observed in the graph of Fig. 26. The varying slopes suggest the different time durations of the heating period between the initial and the peak levels of the process. The data sheet of the graph in Fig. 26 is provided on the CD under the name 'Ramprate-Dewpoint'.

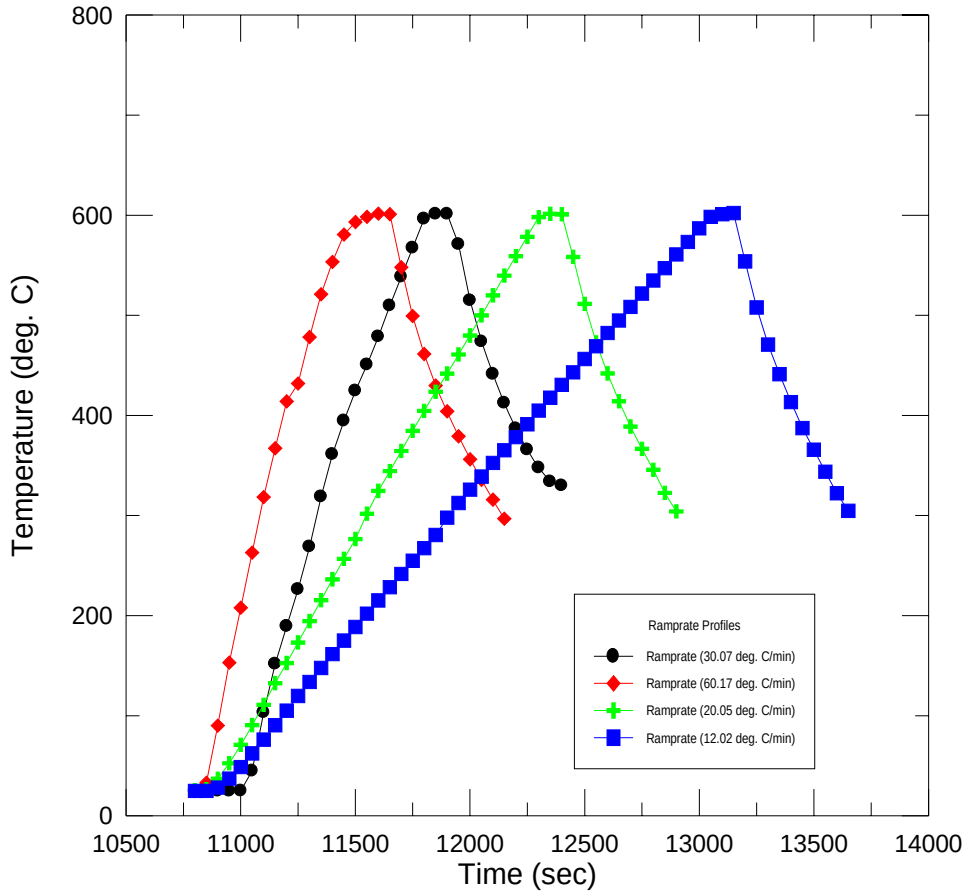

Fig. 26 Ramp-up/dwell/quench history of CAB tests with variable ramp rates

5.3 Results

The graph of Fig. 27 presents the dew point histories of the four experiments. The temperature profiles are also presented. The first observation that could be made form this graph is that during the respective peak brazing periods, the dew point levels have been maintained in each test at the low level regardless of ramp rate which is an essential requirement for getting good outcome of brazing in each case. Also our supposition that the lower ramp rates (higher process time) results in lower amount of vapors available during the peak stages holds well. For example, in the case of $12.02\,^{0}C$ / min ramp rate, the dew point recorded is the lowest. The trend of dew point decrease with the increase of the ramp rates could be clearly observed from the graph. The data of the graph of Fig. 27 are included in the CD under the name 'Ramprate-Dewpoint'.

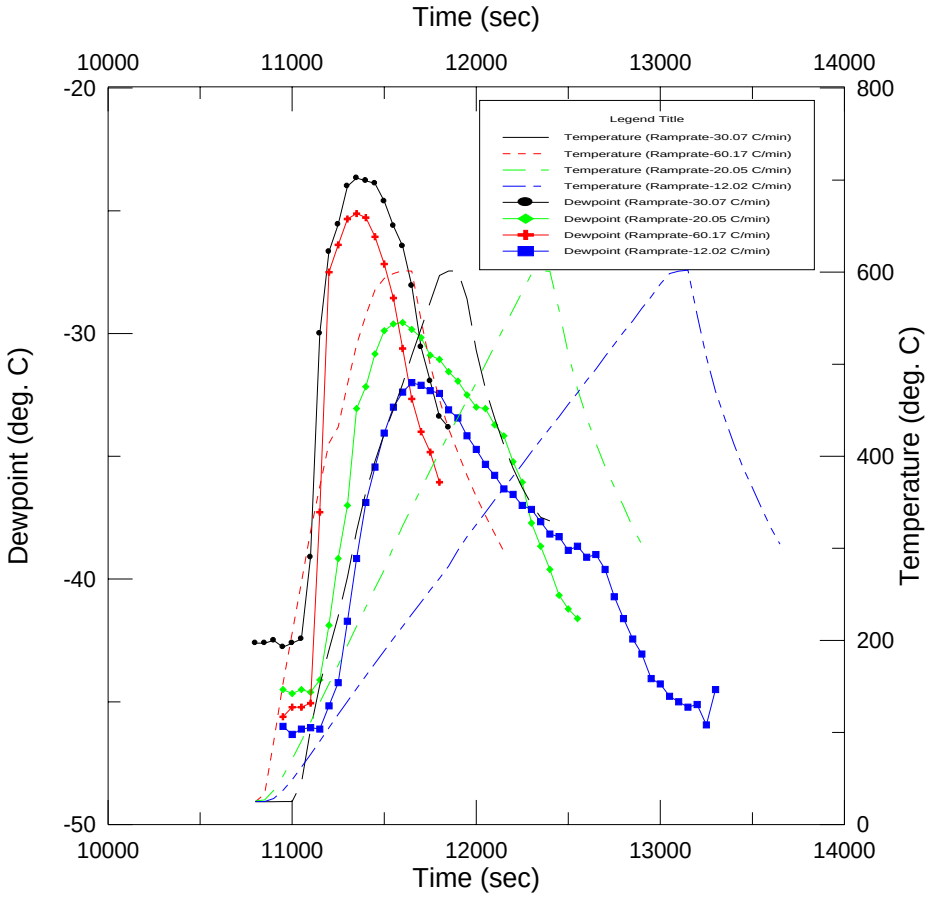

Fig 27: Dew point Histories of Different Ramp-up heating Rates

Table 3: Ramp rates and Joint lengths

Joint Length (mm)	Ramp rates ($^0C/\min$)
30.5	12.02
28.5	20.05
29.5	30.05
31.5	60.17

Table 3: offers data on the measured joint fillet lengths for varying ramp rate tests' samples. Maximum fillet length is obtained in the case of $60.17\,^0C/\min$. Comparing the other three experiments, the trend observed is interesting. As the ramp rates are increased, the joint lengths obtained become high which is quite opposite to the expected influence of dew point trend observed earlier. The reason could be attributed to various factors like the silicon diffusion, amount of flux used, geometric clearance provided. From the explanation given above about the Silicon diffusion, and keeping in mind the various other factors, it is clear that more experimentation has to be performed to find out the optimum heating rates which would result in longer fillet lengths and utilize the benefits of lower dew point levels.

CHAPTER VI

CONCLUSIONS AND FUTURE WORK

Based on performed studies of H_2O emissions and their influence on the product quality in aluminum brazing, the following conclusions can be formulated.

6.1 Conclusions

- Experimental procedures for identification of H_2O release were implemented and reliable data about humidity content were obtained.
- Dew point is an important parameter which indicates the H_2O vapor levels in the background atmosphere during brazing. Steps could be taken to reduce these effluents in order to minimize their effects on the filler metal flow and obtain a good quality brazed joint.
- An aspect of a good quality flux could be identified through the comparison of its dew point temperature history with that of the other fluxes.
- Careful selection of the flux can be done by evaluation of the mass loss of flux during the TGA tests.
- The temperature range of the H_2O exponential release is between 177^0C (the dissociation start point) and the peak stages of the process.
- Flux is the main and primary source for the release of vapors into the surroundings if the controlled atmosphere is maintained properly and products cleaned adequately.
- Ramp rates adjustment can be a potential parameter in reducing the amount of vapors released in the flux, assuming that such modification do not cause other negative effects.

- Slower ramp rates resulted in the lower dew points during the peak brazing stages, but at the same time may adversely influence the joint quality due to a prolonged exposition of products to high temperatures.
- Modeling the process of H_2O release by using the first order reaction assumption for dissociation of H_2O molecules from a flux compound can be used only for initial stages of ramp up heating. The model is too simplistic to capture behavior of the H_2O release at the later stages.

6.2 Future Work

- A more sophisticated model of H_2O release should be developed.
- An extensive additional experimentation with the varying ramp rates should be done to clearly understand their effect on the competing influences of silicon diffusion and other metallurgical effects vs. the influence on H_2O release.
- The art of brazing offers the optimum heating rates that lead to lower dew points at the peak brazing temperatures and at the same time resulting in lower silicon diffusions into base metal. However, a more deterministic science based methodologies for this trade off must be developed.

Appendix A

TGA Data for Sample S

Time, t (sec)	Temperature, T (^0C)	W_{in} (mg)	W_t (mg)	$(0.15 \times W_{in} - W_t)$ (mg)
480	214.5	9.411	9.252	0.024
540	233.9	9.411	9.249	0.024
600	253.6	9.411	9.246	0.025
720	292.9	9.411	9.235	0.027
780	312.7	9.411	9.228	0.027
840	332.6	9.411	9.219	0.029
900	352.4	9.411	9.21	0.030
960	372.3	9.411	9.200	0.032
1020	392.2	9.411	9.187	0.034
1080	412.1	9.411	9.174	0.036
1140	432	9.411	9.162	0.037
1200	452	9.411	9.151	0.039
1260	472	9.411	9.14	0.040
1320	492	9.411	9.126	0.043

Test # 101804

File name on CD TGAS

Refer to Fig. 3

Appendix B

Ln $\dot{m}_{H_2O}$ Vs Time Data for S

Time (sec)	Ln(mh20/1)
480	-3.74
540	-3.71
600	-3.69
660	-3.66
720	-3.63
780	-3.59
840	-3.54
900	-3.5
960	-3.45
1020	-3.39
1080	-3.34
1140	-3.29
1200	-3.24
1260	-3.19
1320	-3.15

Refer to Fig. 22

File name on CD Ln-S

Data for other fluxes is included on the CD attached to this thesis.

Appendix C

Mass of Water vapor from Dew point readings of Sample S

Time, t (sec)	Temperature, T (^0C)	Dew point, T_d (^0C)	Mass of water vapors, $\dot{m}_{H_2O}$ (kg/hr)
0	27	-53.8	1.7614E-06
226	134.5	-47.9	1.80643E-06
315	162.7	-47.2	1.91161E-06
404	190.6	-47.2	2.97497E-06
489	217.4	-43.2	6.32543E-06
575	245.4	-36	1.25055E-05
659	272.7	-29	1.28364E-05
741	299.6	-28.7	1.31751E-05
817	324.9	-28.4	2.0507E-05
892	349.7	-23.6	1.86498E-05
967	374.5	-24.6	1.91233E-05
1038	398.2	-24.4	2.27512E-05
1110	422	-22.4	2.11269E-05
1179	444.9	-23.3	2.13373E-05
1242	465.8	-23.2	2.26395E-05
1304	486.3	-22.5	2.27512E-05

Refer to Fig. 26

File name on CD MFR-S

Appendix D

Mass of Water vapors from TGA and Dew point readings of Sample S

Time, t (sec)	Mass flow rates of water vapor, $\dot{m}_{H_2O}$ (kg/hr) From Model	Mass flow rates of water vapor, $\dot{m}_{H_2O}$ (kg/hr) From Experimental data
226	1.47198E-06	1.7614E-06
315	1.57135E-06	1.80643E-06
404	1.67742E-06	1.91161E-06
489	1.78541E-06	2.97497E-06
575	1.90175E-06	6.32543E-06
659	2.02269E-06	1.25055E-05
741	2.14817E-06	1.28364E-05
817	2.27141E-06	1.31751E-05
892	2.39995E-06	0.000020507
967	2.53578E-06	1.86498E-05
1038	2.67143E-06	1.91233E-05
1110	2.81641E-06	2.27512E-05
1179	2.96272E-06	2.11269E-05
1242	3.10294E-06	2.13373E-05
1304	3.24741E-06	2.27512E-05

Refer to Fig. 26

Appendix E

CAB Experimentation Sample Photographs

Fig. 28 Photograph of Sample using Flux B12

Test # 061706, Refer to Fig. 13

Length of fillet B12-S: 28 mm, B12-L: 18 mm

Fig. 29 Photograph of Sample using Flux BC

Test # 060206, Refer to Fig. 8

Length of fillet BC-S: 29.7 mm, BC-L: 20.1 mm

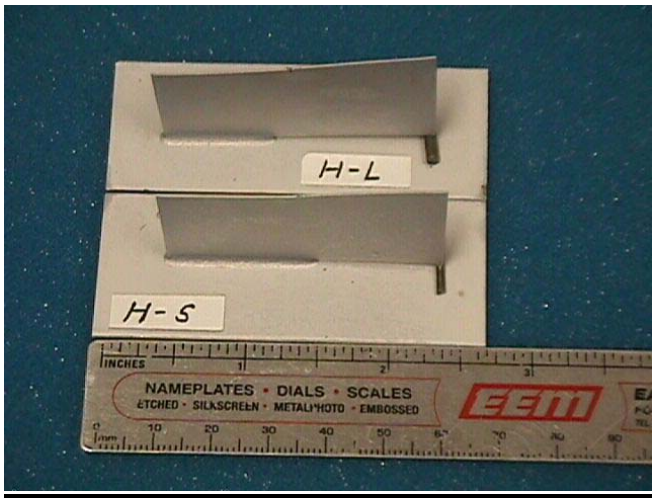

Fig. 30 Photograph of Sample using Flux H

Test # 061506, Refer to Fig. 11

Length of fillet H-S: 27.4 mm, H-L: 21.1 mm

Fig. 31 Photograph of Sample using Flux J

Test # 060106, Refer to Fig. 7

Length of fillet J-S: 26.7 mm, J-L: 19.7 mm

Fig. 32 Photograph of Sample using Flux N

Test # 060306, Refer to Fig. 9

Length of fillet N-S: 28.8 mm, N-L: 20.9 mm

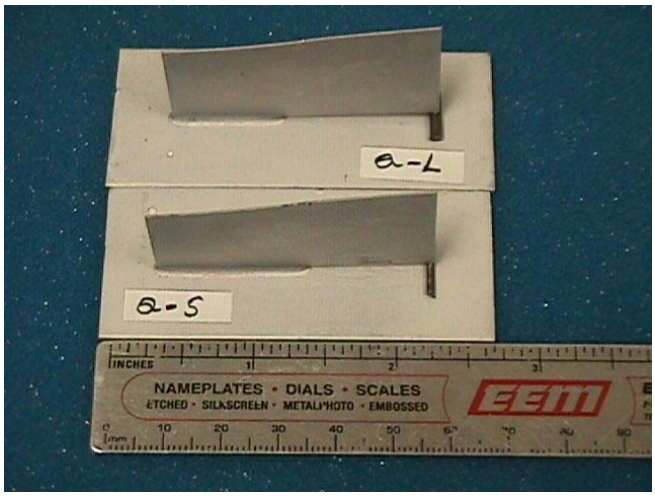

Fig. 33 Photograph of Sample using Flux Q

Test # 061406, Refer to Fig. 10

Length of fillet Q-S: 27.8 mm, Q-L: 21.3 mm

Fig. 34 Photograph of Sample using Flux S

Test # 062006, Refer to Fig. 2

Length of fillet S-S: 28.3 mm, S-L: 20.9 mm

Fig. 35 Photograph of Sample using Flux W

Test # 061606, Refer to Fig. 12

Length of fillet W-S: 25.6 mm, W-L: 20.3 mm

Appendix F

Calculations of Hot Zone Volume Displacements for Different Ramp Rate Experiments

Experiment 1, Test # 030206; Refer to the Fig. 27, Table 2

Ramp rate = $30.07\,^{0}C$ / min

Volumetric flow rate of N_2 gas = $0.02832\,\mathrm{m}^3$ / hr

Volume of the chamber = $0.00259\,m^3$

Time required for N_2 gas to sweep through the whole chamber volume, t_1

$$t_1 = 0.00259/0.02832 \text{ hr}$$

$$= 5.49 \text{ min}$$

Peak brazing temperature = $601.3\,^{0}C$

Time required reaching the peak temperature with $30.07\,^{0}C$ / min ramp rate, T_1

$$T_1 = 601.3/30.07 \text{ min}$$

$$= 19.99 \text{ min}$$

Percentage of chamber volume swept by N_2 gas in 19.99 min, μ_1

$$\mu_1 = (19.99 \times 100)/5.487$$

$$= 364.43\ \%$$

With the above ramp rate, the percentage of the chamber volume swept by the N_2 gas is 364.3% which means the gas sweeps the chamber for approximately 3.69 (≈ 4) times before reaching the peak temperatures.

Experiment 2, Experiment 1, Test # 030306; Refer to the Fig. 27, Table 2

Ramp rate = $20.05\ ^{0}C$ / min

Volumetric flow rate of N_2 gas = $0.02832\,\mathrm{m}^3$ / hr

Volume of the chamber = $0.00259\,m^3$

Time required for N_2 gas to sweep through the whole chamber volume, t_2

$$t_2 = 0.00259/0.02832 \text{ hr}$$

$$t_2 = 0.09145 \text{ hr} = 5.487 \text{ min}$$

Peak brazing temperature = $601.2\,^0C$

Time required reaching the peak temperature with $20.05\,^0C$ / min ramp rate, T_2

$$T_2 = 601.2/20.05 \text{ min}$$

$$= 29.99 \text{ min}$$

Percentage of chamber volume swept by N_2 gas in 29.99 min

$$\mu_2 = (29.99 \times 100)/5.487$$

$$= 546.5\ \%$$

With the above ramp rate, the percentage of the chamber volume swept by the N_2 gas is 546.5% which means the gas sweeps the chamber for approximately 5.46 (≈ 6) times before reaching the peak temperatures.

Experiment 3, Test # 030606; Refer to the Fig. 27, Table 2

Ramp rate = $60.17\,^0C$ / min

Volumetric flow rate of N_2 gas = $0.02832\,\text{m}^3$ / hr

Volume of the chamber = $0.00259\,m^3$

Time required for N_2 gas to sweep through the whole chamber volume, t_3

$$t_3 = 0.00259/0.02832 \text{ hr}$$

$$= 0.09145 \text{ hr} = 5.487 \text{ min}$$

Peak brazing temperature = $601.4\,^0C$

Time required reaching the peak temperature with $30.07\,^0C$ / min ramp rate, T_3

$$T_3 = 601.4/60.17 \text{ min}$$

$$= 9.99 \text{ min}$$

Percentage of chamber volume swept by N_2 gas in 9.99 min, μ_3

$$\mu_3 = (9.99 \times 100)/5.487$$

$$= 182.2\ \%$$

With the above ramp rate, the percentage of the chamber volume swept by the N_2 gas is 182.2% which means the gas sweeps the chamber for approximately 1.82 (≈ 2) times before reaching the peak temperatures.

Experiment 4, Test # 030706; Refer to the Fig. 27, Table 2

Ramp rate = $12.02\,^{0}C$ / min

Volumetric flow rate of N_2 gas = $0.02832\,\mathrm{m}^3$ / hr

Volume of the chamber = $0.00259\,m^3$

Time required for N_2 gas to sweep through the whole chamber volume, t_4

$$t_4 = 0.00259/0.02832 \text{ hr}$$

$$= 0.09145 \text{ hr} = 5.487 \text{ min}$$

Peak brazing temperature = $601.7\,^{0}C$

Time required reaching the peak temperature with $30.07\,^{0}C$ / min ramp rate, T_4

$$T_4 = 601.7/12.02 \text{ min}$$

$$= 50.06 \text{ min}$$

Percentage of chamber volume swept by N_2 gas in 50.06 min, μ_4

$$\mu_4 = (50.06 \times 100)/5.487$$

$$= 912.3\ \%$$

With the above ramp rate, the percentage of the chamber volume swept by the N_2 gas is 364.3% which means the gas sweeps the chamber for approximately 9.12 (≈ 9) times before reaching the peak temperatures.

REFERENCES

1. Field D., Mechanistic Aspects of the Nocolok Flux Brazing Process, SAE Technical Paper Series, 870186, February 23-27, 1987, Michigan.
2. Liu J., Nocolok Flux and Aluminum Brazing, SAE Technical Paper Series, paper # 960244, February 26-29, 1996, Michigan.
3. Laboratory record, Brazing laboratories, UK Center for Manufacturing, Lexington, May-July, 2005.
4. Terrill J.R., Understanding the Mechanisms of Aluminum Brazing can improve results in production operations, Welding Journal, Vol. 50, no.12, pp. 833-839, December, 1971.
5. Takemoto T., Matsunawa A., Decomposition of Non-corrosive Aluminum Brazing Flux during Heating, Journal of Material Science Letters, Vol. 15, pp. 301-303, 1996.
6. Sekulic D.P., Gao F., Zhao H., Zellmer B., Qian Y.Y., Prediction of Fillet Mass and Topology of Aluminum Brazed Joints, Welding Journal-Research Supplement, Vol. 83, no. 3, pp. 102s-110s, March, 2004.
7. Zhang Q., Interaction of Oxide Film with Molten Flux during Aluminum Brazing, Acta Metallurgica Sinica, Vol. 25, no. 2, pp. B121-B124, April, 1989.
8. Culaba A.B., Purvis M.R.I, A Methodology for the Life Cycle and Sustainability Analysis of Manufacturing Processes, Journal of Cleaner Production, Vol. 6, no. 6, pp. 435-445, 1999.
9. Hashemi N., The Effect of Processing Variables on the Microstructures and Properties of Aluminum Brazed Joints, Journal of Material Science, Vol. 37, no. 17, 2002, pp. 3705-3713.
10. Terrill J.R., Diffusion of Silicon in Aluminum Brazing Sheet, Welding Journal, Vol. 45, no. 5, pp. 202S-209S, May 1966.
11. Guzowski M., KB Alloys, Personal communication, 2006.
12. Marlow F., Welding Essentials, Industrial Press Inc., New York, 2001.
13. Claesson E., Engstrom H., Holm T., Scholin., Nitrogen Flow Optimization System for CAB (Nocolok) Furnaces, VTMS Conf., England, May, 1995.

14. NIST Chemistry Web Book (www.nist.gov), date of visit – 08/2006.
15. Zimmer A., Mechanistic Understanding of Aerosol Emissions from a Brazing Operation, AIHAJ, Vol. 61, no. 3, pp. 351-361, May/June 2000.
16. National Institute for Occupational Safety and Health (NIOSH): NIOSH criteria for a recommended standard: Welding, Brazing and Thermal Cutting (DHHS, NIOSH pub no: 88-110), Cincinnati, Ohio: NIOSH, 1988, pp. 25-35, 39-55, 104-111.
17. Bureau of the Census: Detailed population characteristics, In 1980 census of population: Vol. 1, Washington D.C: US Department of commerce, Bureau of the census, 1984.
18. Lashof D., Ahuja D., Relative Contributions of Greenhouse Gas Emissions to Global Warming, Nature, Vol. 344, pp. 529-531, 1990.
19. Karecki S., Pruette L., Beu L., Use of 2H-Heptafluoropropane, 1-Iodoheptafuoropropane, and 2-Iodoheptafluoropropane for a High aspect Ratio via etch in a High Density Plasma Etch Tool, Journal of Vacuum Science and Technology, Vol. 16, July, 1998.
20. Walsh P., Global trends in Diesel Emissions Control, SAE Technical Paper Series, 1999-01-0107, March, 1999.
21. Lewis D.C., Alexeeff G.V., Estimation of Potential Health Effects From Acute Exposure to Hydrogen Fluoride Using a "Benchmark Dose" Approach, Risk Analysis, Vol. 13, no. 1, pp. 13, February 1993.
22. Schwartz M.M., Brazing: For the Engineering Technologist, Chapman & Hill, London, 1995.
23. Sheward G., High Temperature Brazing in Controlled Atmospheres, Pergamon Press Ltd., 1985.
24. Monteith J.L., Lennox J., Principles of Environmental Physics, Edward Arnold, London, 1990.
25. Roberts P.M., Industrial Brazing Practice, CRC Press, Florida, 2004.
26. Takemoto T., Ujie T., Influence of Oxygen Content on Brazeability of a Powder Aluminum Braze, Welding Journal, Vol. 75, no. 11, pp. 372-378, November, 1996.

27. Cooke W. E., Wright T.E., Furnace Brazing of Aluminum with a Non-corrosive Flux, Welding Journal, Vol. 57, no. 12, pp. 23-28, December, 1978.
28. Qiyun Z., "Non-Corrosive Insoluble Flux of Aluminum and its Alloy", Journal of Welding, Vol. 10, no. 2, pp. 3-10, 1995.
29. Shumei Y., Yunhui Z., "The New Progress of Nocolok Flux", Journal of welding technology, Vol. 32, no. 6, pp. 45-47, 2002.
30. Zhang Y., et al. "Study on Potassium Fluoro-aluminate Eutectic Flux", Tianjin Welding Research Institute, Vol. 10, no. 3, pp. 184-186, China.
31. Zhao H., Sekulic D.P., "Isothermal Solidification of Micro Layers of Molten Aluminum Alloys", proceedings of ASME Heat Transfer Conference, 2005.
32. Gao F., Zhao, H.,, Sekulic D.P., Qian, Y., and Walker, L., Solid State Si Diffusion and Joint formation involving Aluminum Brazing sheet", Materials Science and Engineering, Vol. A337, no. 1-2, pp. 228-235, November 2002.
33. Terrill J.R., "Diffusion of Silicon in Aluminum Brazing Sheet", Welding Journal, Vol. 45, no. 5, pp. 202S-209S, May, 1966.
34. Engstroem H., Gullman L.O., Multilayer Clad Aluminum Material with Improved Brazing Properties, Welding Journal, Vol. 67, no. 10, pp. 222S-226S, October, 1988.
35. Gao F., Sekulic D.P., Qian, Y.Y., and Morris, J.G., Formation of Micro Layers of Clad Residue on aluminum Brazing Sheet during Melting and Solidification in Brazing process, Material Science and Technology, Vol. 20, pp. 577 – 584, 2004.
36. Takemoto T., Influence of Oxygen Content on Brazeability of a Powder Aluminum Braze Filler Metal, Welding journal, Vol. 75, no. 11, pp. 372-378, November, 1996.
37. Szargut M., et al., Exergy Analysis of Chemical, Thermal and Metallurgical Processes, Hemisphere Publishing Corporation, New York, 1988.
38. Woodward R., Efficiency, Sustainability and Global Warming, Ecological Ergonomics Vol. 14, pp. 101-111, 1995.
39. Hashemi N., The Effect of Processing Variables on the Microstructures and Properties of Aluminum Brazed Joints, Journal of Materials Science, Vol. 37, no. 17, pp. 3705-3713, September, 2002.

40. Gao F., Zhao H., Sekulic D.P., Solid State Si Diffusion and Joint Formation Involving Aluminum Brazing Sheet, Materials Science and Engineering, Vol. A337, no. 1-2, pp. 228-235, November, 2002.
41. Heldman H., Encyclopedia of Agricultural, Food and Biological Engineering, Marcel Dekker, New York, 2003.
42. Winterbottom W.L., Vacuum Brazing of Aluminum: Auger Studies of Wetting and Flow Characteristics, Journal of vacuum Science and Technology, Vol. 13, no. 2, pp. 634-643, 1976.
43. Hau J., Bhakshi B., Expanding Exergy Analysis to Account for Ecosystem Products and Services, Ohio State University, Environmental Science and Technology, Vol. 38, no. 13, pp. 3768-3777, July 2004.
44. Gutowski T., Environmentally Benign Manufacturing; Product Induced material Flows, Materials Transactions, Vol. 43, no. 3, pp. 359-363, March 2002.
45. Johnson M.R., Environmentally Conscious Manufacturing: A Life Cycle Analysis, 10th ISPE/IFAC International Conference on CAD/CAM, pp. 13-18, 1994.
46. www.wikipedia.org, date of visit – 08/2006.
47. Robert G., The Concept of Environmental Sustainability, Annual review of Ecological Systems, Vol. 26, pp. 1-24, 1995.
48. Sikdhar, S. K., Sustainable Development and Sustainability Metrics, Environmental Protetction Agency, AlChe Journal, Vol. 49, no. 8, pp. 1928-1932, 2003.
49. Sekulic, D.P., University of Kentucky, Lexington, Personal Communication, 2005-06.
50. Stratton, P. F., Successful Furnace Brazing in Controlled Atmospheres, Industrial Heating, Vol. 37, no. 2, pp. 57-59, February, 2006.
51. Swidersky, H. W., Aluminum Brazing with Non-Corrosive Fluxes – State of the Art and Trends in Nocolok Flux Technology, Tagungsband, Hochtemperaturloten und Diffusionschweiben, DVS – Berichte Bd. 212, Dusseldorf: DVS – Verlag, pp. 164-169, 2001,.

52. SECO/ Warwick, Controlled Atmospheric Aluminum Brazing System, Vol. BZ134, pp. 6.
53. Hampston G., Jacobson D.M., Principles of Soldering and Brazing, ASM International, Materials Park, 1993.
54. Nocolok® Flux Material Safety Data Sheet, www.solvaychemicals.com, date of visit 09/2006.
55. Kotz J.C., Chemistry and Chemical Reactivity, Thomson Learning Inc., 2003.
56. Rossini D.F., Chemical Thermodynamics, Wiley, 1899.
57. Sekulic D.P., Sankara J., Advanced Thermodynamic Metrics for Sustainability Assessments of Open Engineering Systems, Thermal Science Journal, Vol. 10, no. 1, pp. 125-140, 2006.
58. Watanabe T., Komatsu S., Development of Flux and Filler Metal for Brazing Aluminum Alloy, Vol. AZ31B, Welding Journal, 2005.
59. Jayasankar S., Exergy Based Method for Sustainable Energy Utilization Analysis of a Netshape Manufacturing System, MS Thesis, UK, 2004.
60. Controlled Atmospheric Brazing Instruction Manual, Centorr Vacuum Industries
61. Thermogravimetric Analysis (TGA), (www.nist.gov), date of visit 08/2006.
62. Kawase, H., et al., Effect of $KAlF_4$ and $K_2AlF_5.H_2O$ Mixtures on Aluminum Brazeability, Journal of Light Metal, Vol. 28, no. 5, pp. 1-5, 1990.
63. Glasby G.P., Sustainable Development: The Need for a New Paradigm, Environment, Development and Sustainability, Vol. 4, pp. 333-345, 2002.
64. Clement D., Oespher R., Inorganic Thermogravimetric Analysis, Elsevier, Amsterdam, New York, 1963.

VITA

Date and Place of Birth

- October 19, 1982 at Vijayawada, Andhra Pradesh, India.

Education

- Bachelor's degree in Mechanical Engineering (B.Tech)
  Nagarjuna University, Guntur, India (2004).

Work Experience

- Research Assistant, Brazing Laboratories, CRMS, UK (April 2005 – June 2005)
- Teaching Assistant, Machining Laboratories, CRMS, UK (Fall 2005)

Conferences

- *11th International Invitational aluminum brazing seminar,* October 24, 2006, AFC- Holcroft, Detroit, MI; The paper presented: Sekulic D.P., Guzowski M., Renduchintala A.B. and Zhao H., "Real Time, In-Situ Monitoring of Joint Formation Involving Isothermal Solidification During Aluminum Brazing", CD Edition.